Submitted to the Special Issue of PAMI on POCV. It was based on a talk at the IEEE Workshop on POCV 2001 and a talk at the Texture02 workshop.

Statistical Modeling and Conceptualization of Visual Patterns

Song-Chun Zhu

Departments of Statistics and Computer Science
University of California, Los Angeles
Los Angeles, CA 90095
sczhu@stat.ucla.edu

Abstract

The objective of perceptual organization (grouping, segmentation and recognition) is to parse generic natural images into their constituent components which are respectively instances of a wide variety of visual patterns. These visual patterns are fundamentally stochastic processes governed by probabilistic models which ought to be learned from the statistics of natural images. In this paper, we review research streams from several disciplines, and divide existing models into four categories according to their semantic structures: *descriptive models, causal Markov models, generative models, discriminative models.* The objectives, principles, theories, and typical models are reviewed in each category. The central theme of this epistemological paper is to study the relationships between the four types of models and to pursue a unified mathematical framework for the conceptualization (or definition) and modeling of various visual patterns. In representation, we point out that the effective integration of descriptive and generative models is the future direction for statistical modeling. To make visual models tractable computationally, we study the causal Markov models as approximations and we observe that the discriminative models are computational heuristics for inferring generative models. Under this unified mathematical framework statistical models for various visual patterns should form a "continuous" spectrum – in the sense that they belong to a serial of probability families in the space of attributed graphs. Visual patterns and their parts are conceptualized as statistical ensembles governed by their models. These statistical models and concepts amount to a visual language with a hierarchy of vocabularies, which is essential for building effective, robust, and generic vision systems.

Keywords: perceptual organization, descriptive models, generative models, causal models, minimax entropy learning, natural image statistics.

1 Introduction

1.1 The quest for a common visual language

The objective of perceptual organization is to parse generic images into their constituent components. For example, figure 1.a shows an image of a football scene which is parsed into a point process (fig1.b), a line and curve process (fig1.c), a uniform region (fig1.d), two texture regions (fig1.e), and two objects – words and human face (fig1.f). The parsing problem is often called *grouping*, *segmentation*, or *recognition* respectively depending on the types of patterns that a task is interested in.

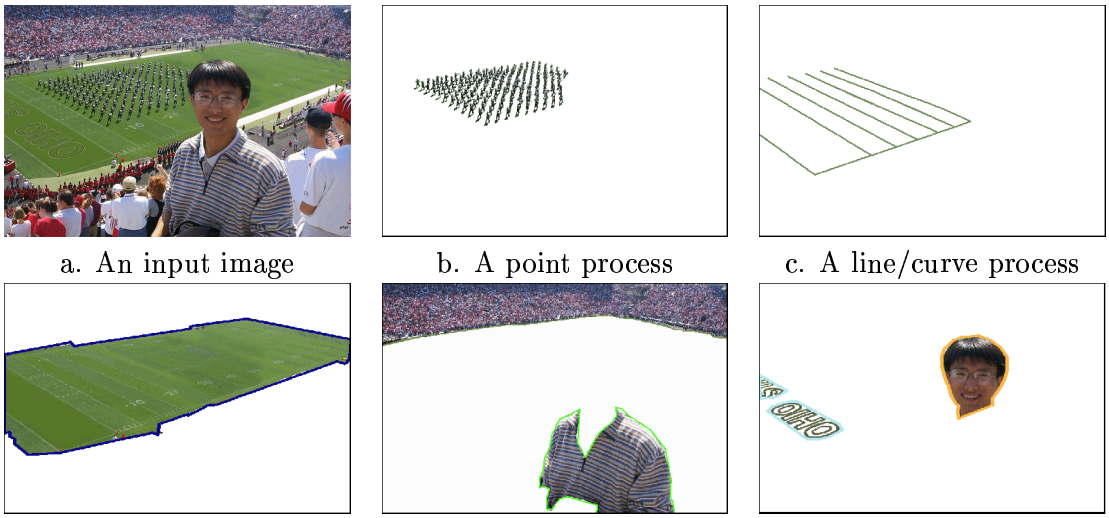

a. An input image b. A point process c. A line/curve process

d. A uniform region e. two texture regions f. objects: face and words

Figure 1: Parsing a generic image into its constituent components which are respectively instances of a wide spectrum of visual patterns in nature. Courtesy of (Tu and Zhu, ECCV 2002).

Given the wide variety of visual patterns in generic images and the diverse stochastic processes that generate them in nature, it is crucial to have *a common vision language* that can represent general visual patterns based on a uniform mathematical framework. More specifically, we pursue a mathematical framework for the following goals.

1. Conceptualization: that is quantitative definition of various visual patterns. For example, what is a "texture"? and what is a "human face"? A visual pattern will be defined on an ensemble of observable signals governed by a statistical model.

2. Learning a visual vocabulary: that is a hierarchy of visual descriptions. For example, pixels, image bases, textons, lines, curves, parts, etc. Compared with the large vocabulary in speech and language (phonemes, words, phrases, and sentences), and the rich structures in physics (atoms, molecules, and polymers), the current visual vocabulary is far from being sufficient. It is of particular difficulty to learn the vocabulary at low level vision (or early vision in a psychophysical term), like textons, because human vision processes these descriptions unconsciously, and they

constitute the richest stochastic patterns in natural images. But what are the "visual atoms"? How do we define them quantitatively?

3. Statistical modeling: pursuing informative and non-accidental *features and statistics* from the ensemble of natural images which characterize the spatial relationships between the visual descriptions, and learning probabilistic models that account for the features and statistics. These models govern the statistical ensemble and thus they are consistent with the definitions of the patterns. Furthermore, the models for various visual patterns, ranging from textures to geometric shapes, should form a "continuous spectrum" in the sense that they are from a series of nested probability families. What are the mathematical space for these models and patterns?

4. Computational tractability. There will be a broad range of models, from appearance models on raw images to physics models on low dimensional hidden structures, which can all characterize a visual pattern. The choice of models and their approximations should facilitate effective inference for the purpose of the task. Model selection is a daunting task especially we presently cannot formulate quantitatively the purpose of generic vision. In the paper, we distinguish our visual knowledge into two kinds of models. One is *representational model*, such as the descriptive models and generative models, and the other is *computational model*, such as the discriminative models. The latter are computational heuristics for inferring the representational models. Then what are the intrinsic relationships between these representational and computational models?

The questions above have motivated long threads of research from many disciplines, for example, applied mathematics, statistics, computer vision, image coding, psychology, and computational neurosciences. Recently a uniform mathematical framework emerges from the interactions between the research streams and experimentally a large number of visual patterns can be modeled realistically. This inspires the author to write an *epistemology* paper to summarize the progress in the field and report our current understandings of the big questions above. The objective of the paper is to facilitate communications between different fields and provides a road map for the pursuit of a common visual language.

1.2 Plan of the paper

The paper starts with a survey of the literature in section (2) to set the background. We divide the literature in four research streams: 1) the study of natural image statistics, 2) the analysis of natural image components, 3) the grouping of natural image elements, and 4) the modeling of visual patterns. These streams result in four types of models: descriptive, generative, causal Markov, and discriminative as we shall discuss in section (2).

The relationships of the four types of models are the following. A visual pattern is either represented by a descriptive (Markov) model or by a generative model. Then it is shown that the descriptive and generative models are inseparable and they ought to be integrated and learned under a unified principle. In the literature, a generative model often includes a trivial descriptive model, and a descriptive model often has a trivial generative assumption. *The effective integration*

of the descriptive and generative models shall lead to richer classes of hierarchic visual models and thus is viewed, in this paper, as the future direction of visual modeling. A causal Markov model is an approximation to a descriptive model, and is a special case for computational convenience. Finally a discriminative model represents computational heuristics for inferring generative models. *The effective interaction between the integrated generative/descriptive models and discriminative models is the future direction, according to this paper, for developing computationally tractable algorithms for inference.*

This unifying picture makes it clear how different research streams tackles the problem from different representational and computational perspectives.

Section (3) presents a common maximum likelihood formulation for modeling visual patterns. Then it leads to the choice of two families of the probability models: descriptive models and generative models. Then the paper presents the descriptive and generative models in parallel.

Section (4) presents the basic assumptions and principles for learning descriptive models, and seven typical examples from low level pattern to high level patterns in the literature. Section (5) presents the statistical physics foundation of descriptive models and three types of ensembles: the micro-canonical, canonical, and grand-canonical ensembles. Then we conceptualize a visual pattern to an ensemble of physical states.

In parallel, Section (6) presents the basic assumptions, methods, and five typical examples for learning generative models. Section (7) revisits the conceptualization of patterns from the perspectives of generative models, and states that the visual vocabulary can be learned as parameters in the generative models.

Then the paper turns to computational issues. In Section (8) we discuss a few causal Markov models as approximations to descriptive models and special cases. In section (9), we study how discriminative models can be used for inferring hidden structures in generative models.

Finally Section (10) concludes the paper by raising some challenging issues in model selection and the balance between descriptive and generative models.

2 Literature survey — a global picture

In this section, we briefly review four research streams and summarize four types of probabilistic models to set a global picture.

2.1 Four research streams

Stream 1: the study of natural image statistics.

It is now widely accepted that generic vision systems, biologic or machine, should be tuned to the ensemble of natural images, and thus it is of great importance to study the statistical properties of natural images. Most of the early work studied natural image statistics from the perspective of image coding and redundancy reduction, and often use them to predict/explain the neuron

responses.

In history, Attneave (1954), Barlow (1961), and Gibson (1966) were among the earliest who argued for the ecologic influence on vision perception. Kersten (1987) did perhaps the first experiment measuring the conditional entropy of the intensity at a pixel given the intensities of its neighboring pixels, in a spirit similar to Shannon's (1948) experiment of measuring the entropy of English words. Clearly the strong correlation of intensities between adjacent pixels results in low entropy. Further study of the intensity correlation in natural images leads to an interesting re-discovery of a $1/f$ power law by Field (1987).[1] By doing a Fourier transform on natural images, the amplitude of the Fourier coefficients at frequency f (averaged over orientations) fall off in a $1/f$-curve (see Figure 4.a). The power may not be exactly $1/f$ and vary in different image ensembles (Ruderman, 1994). This inspired a large body of work in biologic vision and computational neurosciences which study the correlations of not only pixel intensities but responses of various filters at adjacent locations. These work also expand from grey level static images to color and motion images (see Atick et al 1992, Simoncelli et al 2001 for details).

Meanwhile, the study on natural image statistics extends from correlations to histograms of filter responses, for example, Gabor filters.[2] This leads to two interesting observations. One observation is that the histograms of filter responses on natural images have high kurtosis (Field, 1994). This reveals that natural images have high order (non-Gaussian) structures. The second discovery was reported independently by (Ruderman, 1994) and (Zhu and Mumford 1996-97) that the histograms of gradient images are consistent over scales (see Fig. 5). The scale invariance experiment is repeated by several teams (Chi and S.Geman 1998, Grenander and Srivastava, 2001). Further studies along this direction include investigations on joint histograms and low dimensional manifolds in high dimensional spaces. For example, the density on a 7-D unit sphere for all 3×3 pixel patches of natural images (Lee, Huang, and Mumford, 2000, Koloydenko and D.Geman 2000). Going beyond pixel statistics, some most recent work measured the statistics of object shapes (Zhu, 1999), contours (Geisler et al. 2001), and the size of regions and objects in natural images (Alvarez, Grousseau, and Morel 1998).

Stream 2: the analysis of natural image components

The high kurtosis in image statistics observed in stream 1 is marginal evidence for hidden structures in natural scenes. A classic way for discovering structures and reducing image redundancy is to transform an image into a superposition of image components or atomic bases. The transforms achieve two nice properties. 1). The coefficients of these bases are less correlated or independent in ideal cases. 2). The number of bases for approximately reconstructing an image is often much

[1] The spectra power-law was firstly reported in (Deriugin, 1957) in studying television signals, and re-discovered by (Cohen and Carlson et al, 1975-78) in photographic analysis, and then Burton and Moorhead, 1987) in optics study. It was Fields' work that brought it to attention of the broad vision communities.

[2] Correlations only measures second order moments while histograms include all the high order information, such as skewness (third order) and kurtosis (fourth order).

smaller than the number of pixels, i.e. dimension reduction. For example, Fourier transform, wavelet transforms (Mallat 1989, Coifman and Wickerhauser 92), and various image pyramids (Simoncelli et al 1992) for generic images, and principal component analysis for some specific ensembles of images.

If one treats an image as a continuous function, then a mathematical tool for decomposing images is *harmonic analysis* (see Meyer 1985, 1988, Donoho etc 1998). Harmonic analysis is concerned with decomposing various classes of functions (i.e. mathematic spaces) by different bases. Further development along this vein includes the wedgelets, ridgelet, edgelets, curvelets by Donoho and Candes in a series of papers.

Most recently, two ideas from this research stream are most inspiring. One is *sparse coding* with *over-complete basis or dictionary*. With over-complete basis, an image may be reconstructed by a small (sparse) number of bases in the dictionary. This often leads to 10-100 folds of dimension reduction. For example, an image of 200×200 pixels can be reconstructed approximately by about $100 - 500$ base images. The second idea is that the optimal basis should be learned from (or tuned to) the ensemble of natural images. The two insights are combined in (Olshausen and Field, 1996). Figure 13 shows some bases learned from a set of natural images. Added to this development is the independent component analysis (ICA) (Common 1994, VanHateren and Ruderman 1998). It is shown in harmonic analysis that the Fourier, wavelet, and ridgelet bases are independent components for various ensembles of mathematical functions (see Donoho et al 1998 and ref. therein). But for the ensemble of natural images, it is not possible to have an independent basis, and one can only compute a basis which maximize some measure of independence.

Stream 3: the grouping of natural image elements

The third research stream originated from Gestalt psychology (Koffka, 1935). Human visual perception has strong tendency (bias) towards forming global percept ("whole" or pattern) by grouping local elements ("parts"). For example, Human vision completes illusory figures, and perceives hallucinatory structures from totally random dot patterns (Smith, 1986). In contrast to research streams 1 and 2, early work in stream 3 focused on *computational procedures and algorithms* that seemed to demonstrate performance similar to human perception. This includes work on illusory figure completion and grouping from local edge elements (Guy and Medioni 1996).

While the Gestalt laws are quite successful in many artificial illusory figures, their applicability in real world images was haunted by ambiguities. A pair of edge elements may be grouped in one image but separated in the other image, depending on information which may have to be propagated from distant edge elements. So the Gestalt laws are not really *deterministic laws* but rather *heuristics* or *importance hypotheses* which are better used with probabilities.

Lowe (1985) was the first who computed the likelihoods (probabilities) for grouping a pair of line segments based on proximity, co-linearity, or parallelism respectively. Considering a number of line segments that are independently and uniformly distributed in terms of lengths, locations

and orientations in a unit square, Lowe estimated the expected number for a pair of line segments at a certain configuration that are formed *accidentally* according to this uniform distribution. Lowe conjectured that the likelihood of grouping a pair of line segments in real images should be proportional to the inverse of this expected number – which he called *non-accidental property*. In a similar method, Jacobs (1993) calculated the likelihood for grouping a convex figure from a set of line segments.

People also used Bayes networks (see Fig 19) to compute and propagate probabilities in grouping elements (Sarkar and Boyer, 1993) and generic object recognition (Dickinson et al. 1992). Bienenstock, Geman, and Potter (1997) proposed a compositional vision approach for grouping of handwritten characters. Moisan, Desolneux and Morel (2000) compute the likelihoods for meaningful alignments.

Stream 4: the modeling of natural image patterns

By the end, all studies boil down to the explicit modeling of image patterns. Theoretically speaking, mathematical models of patterns must agree with (or reproduce) the observed image statistics (stream 1) and characterize the distributions of image components (stream 2). As we shall show in late section, the grouping heuristics in streams 3 are for effective inference of the models of pattern.

In the literature, Grenander (1976), Cooper (1979), and Fu (1982) were the pioneers using statistical models for various visual patterns. In the late 1980s and early 1990s, image models become popular and indispensable when people realized that vision problems, typically the shape-from-X problems, are fundamentally ill-posed. Extra information is needed to account for regularities in real world scenes. The early models all assumed simple *smoothness* (sometimes piecewisely) of surfaces or image regions, and they were developed from different perspectives. For example, physically-based models (Terzopoulos, 1983, Blake and Zisserman, 1987), regularization theory (Poggio, Torre, and Koch, 1985), energy functionals (Mumford and Shah, 1989). Later these concepts all converged to statistical *a priori* models which prevailed due to two pieces of influential work. The first work is the Markov random field (MRF) modeling (Besag, 1973, Cross and Jain, 1983) introduced from statistical physics. The second work is the Geman and Geman (1984) paper which showed that vision inference can be done rigorous by Gibbs sampler under the Bayesian framework. There were extensive literature on Markov random field ideas and Gibbs sampling in later 1980s. This trend went down in the early 1990s for two practical reasons. 1). Most of those Markov random field models are based on pair cliques and thus do not realistically characterize natural image patterns. 2). The Gibbs sampler is computationally very demanding on such problems.

Other probability models of visual patterns include deformable templates for objects, such as human face (Yuille, 1991) and hands (Grenander et al 1991). The deformable templates are also MRF models. In contrast to the homogeneous MRF models mentioned above, deformable templates are inhomogeneous on small graphs whose nodes are labeled. We should return to more recent MRF

models in later section.

2.2 Four categories of statistical models

More concretely, the interactions of different streams resulted in four categories of probability models. In the following, we briefly review the four types of models to set background for a mathematical framework that unifies them.

Category 1. Descriptive models.

Firstly, the integration of stream 1 and stream 4 yields a class of models which we call "descriptive models". Given an image ensemble and its statistics properties, such as the $1/f$-power law, scale invariant gradient histograms, one can alway construct a probability model which produces the observed statistics. The probability is of the Gibbs (MRF) form following a maximum entropy principle (Jaynes, 1957). We call such models the descriptive models because they are constructed based on statistical descriptions of the image ensembles.

The attraction of descriptive model is that a single probability model can integrate all statistical measures of different image features. Such integration is not a simple product of the likelihoods or marginals on different features but uses sophisticated energy functions to account for the dependency of these features. Furthermore the descriptive models are least biased, and this provides a way to exactly measure the "non-accidental statistics" sought after by Lowe (1987). We shall deliberate on this point in latter section.

The descriptive models are all built on certain graph structures including lattices. There are four variants of descriptive models in the literature. 1). *Homogeneous models* where the statistics are assumed to be the same for all elements (vertices) in the graph. The random variables are the attributes of vertices, such as pixel intensities. 2). *Inhomogeneous model* where the elements (vertices) of the graph are labeled, and different features and statistics are used at different sites. 3). *Mixed Markov models* where the graph structures (adjacency and neighborhood) are not predefined and are subject to stochastic inference. Thus mixed Markov models engages some addressing variables in addition to the attribute variables (Mumford, 1995). 4). *Random graph models* where the number of vertices and their neighborhood structures in the graph are all random variables. Descriptive models are sufficient to model all visual patterns. These models are unified under the minimax entropy framework (Zhu, Wu, Mumford, 1997), and they differ in the types of elements, the statistics between the elements, and the graph structures.

Category 2. Causal Markov random field (MRF) models and energy approximations

The descriptive models are often computationally expensive, especially for low level models, due to the difficulty of computing the partition (normalizing) functions in Gibbs models. This problem becomes prominent when the descriptive models have large image structures and account for high order image statistics. In the literature, two approaches attempt to get around the partition functions through approximation.

One approach uses causal MRF models. A causal MRF model approximates a descriptive model

by imposing a partial (or linear) order among the vertices of the graph such that the joint probability can be factorized as a product of conditional probabilities. The latter have lower dimensions and thus are much easier to learn and to compute. The Causal MRF models are still maximum entropy distributions subject to, sometimes, the same set of statistical constraints as the descriptive models. But the entropy is maximized in a limited probability space.

The other approach still uses undirected graph structure, but it introduces a *belief* at each vertex. These beliefs are only normalized at single site or a pair of sites, and they do not necessarily form a legitimate (well normalized) joint probability for the whole graph. Thus it avoids computing the partition functions at all. This technique, originated in statistical physics, includes the mean field approximation, the Bethe and Kikuchi approximations (see Yedidia et al. 2000 and Yuille, 2001).

Category 3. Generative models

The principled way to tackling the computational complexity of descriptive models (and to other vision purposes) is to introduce hidden variables that can "explain away" the strong dependency in observed images. This leads to hierarchic generative models (Dayan et al 1995, Frey and Jojic, 1999). For example, the sparse coding scheme (Olshausen and Field, 1997) is a typical generative model which assumes an image being generated by a small number of bases. The computation becomes less intensive because of the reduced dimensions and the less dependency between the hidden variables, i.e. they are often partially de-coupled.

Intuitively, when there are strong dependency in observed signals (say images), they form low dimensional manifolds embedded in very high dimension space. For example, the image of a circular disk may have only three degrees of freedom (DOF) (i.e. x,y,r), and thus all disk images ($n \times n$ pixels) span only a 3D manifold in R^{n^2}. Thus a Markov chain sampling the image density consistently falls off the manifold if it walks in the dimensions of the pixel intensities, and thus leads to extremely frustration. By introducing the hidden variables it can walk effectively along the dimensions of the manifold itself.

The generative models are not separable from descriptive models, because the hidden variables at the root are not further generated by other variables and must be characterized by a descriptive model, though in the literature the latter may often be a trivial iid Gaussian model or a causal Markov model. For example, the sparse coding scheme is a two layer generative model and assumes the image bases are iid hidden variables, and hidden Markov models in speech and motion is a two layer model whose hidden layer is a Markov chain (causal MRF model with linear order). In visual modeling, the hidden variables must be characterized by more general descriptive models (see later section).

We argue that the effective integration of descriptive and generative models is the right way for visual modeling because it leads to the discovery of a visual language and vocabulary and computationally tractable models.

Category 4. Discriminative models

The grouping probabilities used in stream 3 are mostly discriminative models. In compari-

son, descriptive models and generative models are used as prior probabilities and likelihoods in the Bayesian framework, while discriminative models approximate posterior probabilities of hidden variables (often individually) based on local features. Strictly speaking, the discriminative probabilities are not representational models but computational heuristics for inferring the hidden variables in generative models. As we shall show in later section that they are *importance proposal probabilities* which drive the stochastic Markov chain search for fast convergence. It was shown, through simple case, that the better the proposal probability approximate the posterior, the faster the algorithm converges (Mengersen and Tweedie, 1994).

The interaction between discriminative and generative models has not gone very far in the literature. Recent work include the data driven Markov chain Monte Carlo (DDMCMC) algorithms for image segmentation, parsing, and object recognition (Tu and Zhu et al 2000-02).

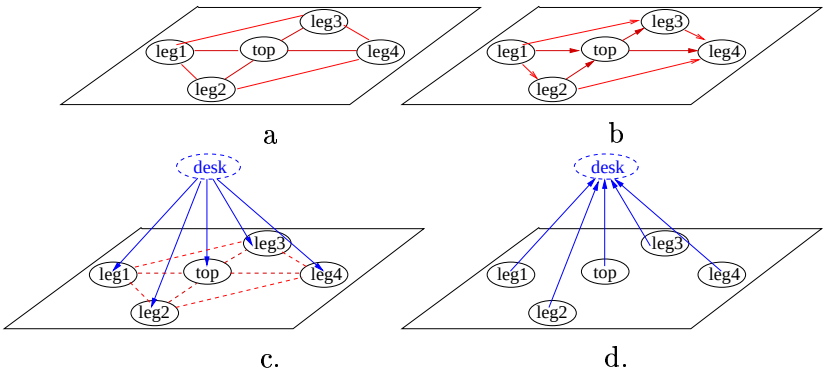

Figure 2: Four types of models for a simple desk object. a). descriptive (MRF), b). causal MRF, c). generative + descriptive d). discriminative.

Summary and justification of terminology

To clarify the terminology, Figure 2 shows a trivial example of the four models for a desk. A desk consists of four legs and a top, denoted respectively by variables d, l_1, l_2, l_3, l_4, t for their attributes. Figure 2.a shows the undirected graph for a descriptive model $p(l_1, l_2, l_3, l_4, t)$. It is in the Gibbs form with a number of energy terms to account for the spatial arrangement of the five pieces. Intuitively, this descriptive model just accounts for the phenomological probability that the five pieces occur together without "understanding" a hidden concept of chair – denoted by the hidden variable d. The causal MRF model assumes a directed graph in Figure 2.b. Thus it simplifies the descriptive model as $p(l_2)p(t|l_1, l_2)p(l_3|t, l_1)p(l_4|t, l_2, l_3)$. Figure 2.c is a two level generative model which involves a hidden variable d for the "whole" desk. The desk generates the five pieces by a model $p(l_1, l_2, l_3, l_4, t|d)$. d may consist of global attributes of the desk which controls the positions of the five parts. If we assume that the five pieces are conditionally independent, then it becomes a context free grammar (without the dashed lines). In general, we still need a descriptive model to characterize the spatial deformation by a descriptive model (see the dashed links). But this new descriptive model $p(l_1, l_2, l_3, l_4, t|d)$ is much less complicated than $p(l_1, l_2, l_3, l_4, t)$ in Figure 2.a.

Finally Figure 2.d is a discriminative model, the links are pointed from parts to whole (reversing the generative arrows). It tries to compute a number of posterior probabilities $p(d|t)$, $p(d|l_i), i = 1, 2, 3, 4$. These probabilities are often treated as "votes" which are then summed up in a generalized Hough transform.

Syntactically the generative, causal Markov, and discriminative models can be called Bayesian (causal, belief) networks as long as there are no loops in the graphs. But this is very confusing in the literature. Our terminology is from a semantic perspective. We call it a generative model if the links are directed downwards in the conceptual hierarchy, a discriminative model if the links are upwards (also see Figure 19), and a causal MRF model if the links are pointed to variables at the same conceptual level (also see Figure 17). For example we consider hidden Markov models in motion or speech as two layer models where the hidden variables is governed by a causal Markov (descriptive) model because they belong to the same semantic level.

3 Problem formulation

Now we start with a general formulation of visual modeling as statistical learning.

Let $\mathcal{E}$ denote the ensemble of natural images in our environment. As the number of natural images is so large, it makes sense to talk about a frequency $f(\mathbf{I})$ for images $\mathbf{I} \in \mathcal{E}$.[3] $f(\mathbf{I})$ is intrinsic to our environment and our sensory system. For example, $f(\mathbf{I})$ would be different for fish living in deep ocean or rabbits living in prairie, or if our vision is 100 times more acute. The general goal of visual modeling is to estimate the frequency $f(\mathbf{I})$ by a probabilistic model $p(\mathbf{I})$ based on a set of observations $\{\mathbf{I}_1^{\text{obs}}, ..., \mathbf{I}_M^{\text{obs}}\} \sim f(\mathbf{I})$. It may sound quite ridiculous to estimate a density like $f(\mathbf{I})$ which is often in 256×256 space. But as we shall show in the rest of the paper, this is possible because of the strong regularities in natural images, and easy access to a very large number of images. For example, if a child sees 20 images per second, and open eyes 16 hours a day, then by the age of ten, he/she has seen 3 billion images.

The probability model $p(\mathbf{I})$ should approach $f(\mathbf{I})$ by minimizing a Kullback-Leibler divergence $KL(f||p)$ from f to p,

$$KL(f\,||\,p) = \int f(\mathbf{I}) \log \frac{f(\mathbf{I})}{p(\mathbf{I})} d\mathbf{I} = E_f[\log f(\mathbf{I})] - E_f[\log p(\mathbf{I})]. \tag{1}$$

Approximating the expectation $E_f[\log p(\mathbf{I})]$ by a sample average leads to the standard maximum likelihood estimator (MLE),

$$p^* = \arg\min_{p \in \Omega_p} KL(f\,||\,p) \approx \arg\max_{p \in \Omega_p} \sum_{m=1}^{M} \log p(\mathbf{I}_m^{\text{obs}}), \tag{2}$$

where Ω_p is the family of distributions where p^* is searched for. One general procedure is to search for p in a sequence of nested probability families,

$$\Omega_0 \subset \Omega_1 \subset \cdots \subset \Omega_K \to \Omega_f \ni f,$$

[3] When the image lattice is large enough, the effects of boundary conditions can be ignored.

where K indexes the dimensionality of the space, e.g. the number of free parameters. As K increases, the probability family should be general enough to approach f to an arbitrary preset precision.

There are two choices for the families Ω_p in the literature.

The first choice is the descriptive model. They are called exponential or log-linear models in statistics, and Gibbs models in physics. We denote them by

$$\Omega_1^d \subset \Omega_2^d \subset \cdots \Omega_K^d \to \Omega_f. \tag{3}$$

The dimension of the space Ω_i^d is augmented by increasing the number of *feature statistics* of $\mathbf{I}$.

The second choice is the generative model, or mixture models in statistics, denoted by

$$\Omega_1^g \subset \Omega_2^g \subset \cdots \subset \Omega_K^g \to \Omega_f \ni f. \tag{4}$$

The dimension of Ω_p is augmented by introducing hidden variables for the underlying image structures in $\mathbf{I}$.

Both families are general enough for approximating any distribution f. In the following sections, we deliberate on the descriptive and generative models and learning methods, and then discuss their unification and the philosophy of model selection.

4 Descriptive modeling

In this section, we review the basic principle of descriptive modeling, and show a spectrum of seven examples for modeling visual patterns from low to high level.

4.1 The basic principle of descriptive modeling

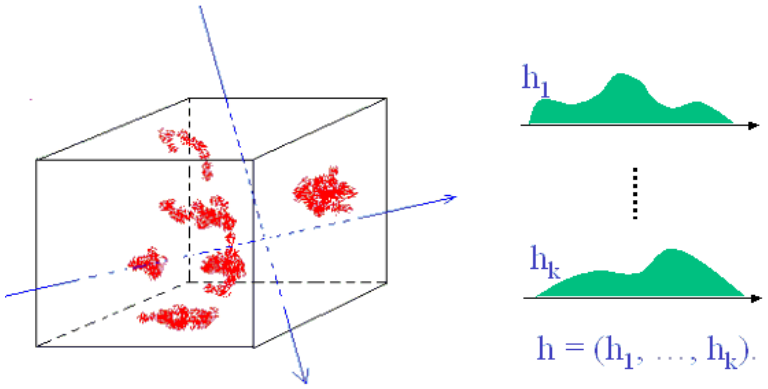

Figure 3: Descriptive modeling: estimating a high dimensional frequency f by a maximum entropy model p that matches the low dimensional projections of f. The projections could be non-linear.

The basic idea of descriptive modeling is shown in Figure 3. Let $\mathbf{s} = (s_1, ..., s_n)$ be a representation of a visual pattern. For example $\mathbf{s} = \mathbf{I}$ could be an image with n pixels, and in general $\mathbf{s}$ is a list

of attributes for vertices of a random graph. An observable data ensemble is illustrated by a cloud of points in an n-space, and each point is an instance of the visual pattern. A descriptive method extracts a set of K **features** as *deterministic transforms* of $\mathbf{s}$, denoted by $\phi_k(\mathbf{s}), k = 1, ..., K$. For example, $\phi_k(\mathbf{I}) =< F, \mathbf{I} >$ is a projection of image $\mathbf{I}$ on a linear filter (say Gabor) F. These features (such as F) are illustrated by axes in Figure 3. In general, the axes don't not have to be straight lines and could be more than one dimensional. Along these axes we can compute the projected histograms of the ensemble (the right side of Figure 3). We denote these histograms as $\mathbf{h}_k^{\text{obs}}$ for features $\phi_k(\mathbf{s}), k = 1, 2, ..., K$. They are estimates to the marginal statistics of $f(\mathbf{s})$.

A model p must match the marginal statistics $\mathbf{h}_k^{\text{obs}}, k = 1, ..., K$ if it is to estimate $f(\mathbf{s})$. Thus, we have descriptive constraints:

$$E_p[h(\phi_k(\mathbf{s}))] = \mathbf{h}_k^{\text{obs}} \approx E_f[h(\phi_k(\mathbf{s}))], \quad k = 1, ..., K. \tag{5}$$

The least biased model that satisfies the above constraints is obtained by maximum entropy (Jaynes, 1957), and this leads to the FRAME model (Zhu, Wu, and Mumford, 1996-97),

$$p_{\text{des}}(\mathbf{s}; \boldsymbol{\beta}) = \frac{1}{Z(\boldsymbol{\beta})} \exp\{- \sum_{k=1}^{K} < \boldsymbol{\lambda}_k, h(\phi_k(\mathbf{s})) >\}. \tag{6}$$

The parameters $\boldsymbol{\beta} = (\boldsymbol{\lambda}_1, ..., \boldsymbol{\lambda}_K)$ are Lagrange multipliers and they are computed by solving the constraint equations (5). $\boldsymbol{\lambda}_k$ is a vector whose length is equal to the number of bins in the histogram $h(\phi_k(\mathbf{s}))$. As the features $\phi_k(\mathbf{s}), k = 1, 2, ..., K$ are often correlated, the parameters $\boldsymbol{\beta}$ are learned to weight these features. Thus $p_{\text{des}}(\mathbf{s}; \boldsymbol{\beta})$ integrates all the observed statistics. [4]

The selection of features in p_{des} is guided by a minimum entropy principle. For any new feature ϕ^+, we can define its non-accidental statistics following (Zhu, Wu, and Mumford, 1997).

Definition 1 *:* **(non-accidental statistics)**. *Let* $\mathbf{h}_f^+$ *be the observed statistics for a novel feature* ϕ^+ *computed from the ensemble, i.e.* $\mathbf{h}_f^+ \approx E_f[h(\phi_+(\mathbf{s}))]$ *and* $\mathbf{h}_p^+ = E_{p_{\text{des}}}[h(\phi_+(\mathbf{s}))]$ *its expected statistics according to a current model* p_{des}*. Then the non-accidental statistics of* ϕ^+ *with respect to the previous* K *features is a quadratic distance* $d(\mathbf{h}_f^+, \mathbf{h}_p^+)$.

$d(\mathbf{h}_f^+, \mathbf{h}_p^+)$ measures the statistics discrepancy of ϕ^+ which are not captured by the previous K features. Let p_{des}^+ be an augmented descriptive model with the K statistics in p_{des} plus the feature ϕ^+, then the following theorem is observed in (Zhu, Wu, and Mumford, 1997).

Theorem 1 (Feature Pursuit). *In the above notation,*

$$d(\mathbf{h}_f^+, \mathbf{h}_p^+) = KL(f \,||\, p_{\text{des}}) - KL(f \,||\, p_{\text{des}}^+) = \text{entropy}(p_{\text{des}}) - \text{entropy}(p_{\text{des}}^+), \tag{7}$$

where $d(\mathbf{h}_f^+, \mathbf{h}_p^+)$ *is a quadratic distance between the two histograms.*

[4] In natural language processing, such Gibbs model was also used in modeling the distribution of English letters (Della Pietra, Della Pietra, and Lafferty 1997).

The higher the non-accidental statistics, the more informative feature ϕ^+ is for the visual pattern. Thus a feature ϕ^+ is selected sequentially by a minimax entropy principle following equation (7).

The Cramer and Wold theorem states that the descriptive model p_{des} can approximate any densities f using linear axes only (also see [90]).

Theorem 2 (Cramer and Wold) *Let f be a continuous density, then f is a linear combination of $\mathbf{h}$, the latter are the marginal distributions on the linear filter response $F^{(\xi)} * \mathbf{s}$, and f can be reconstructed by p_{des}.*

4.2 A spectrum of descriptive models for visual patterns

In the past few years, the descriptive models have successfully accounted the observed natural image statistics (stream 1) and modeled a spectrum of visual patterns displayed in fig. 1.

1. Descriptive model for $1/f$-power law of natural images

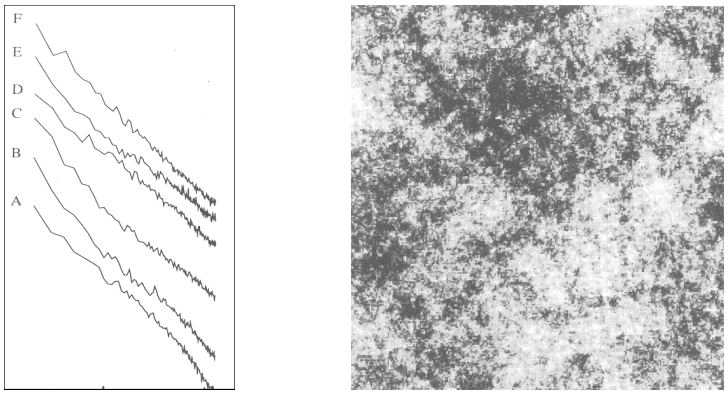

a b

Figure 4: a). The log-Fourier-amplitude of natural images are plotted against $\log f$. Courtesy of (Field, 1987). b). A randomly sampled image with $1/f$ Fourier amplitude. Courtesy of (Mumford, 1995)

An important discovery in studying the statistics of natural images is the $1/f$ power-law (stream 1). Let $\mathbf{I}$ be a natural image and $\hat{\mathbf{I}}(\xi, \eta)$ its Fourier transform. Let $A(f)$ be the Fourier amplitude $|\hat{\mathbf{I}}(\xi, \eta)|$ at frequency $f = \sqrt{\xi^2 + \eta^2}$ averaged over all orientations, then $A(f)$ falls off in a $1/f$-curve.

$$A(f) \propto 1/f, \quad \text{or} \quad \log A(f) = \text{const} - \log f.$$

Figure 4.a is a result in logarithmic scale by Field (1987) for six natural images. The curves are fit well by straight lines in log-plot. This observation reveals that natural images contain equal Fourier power at each frequency band – scale invariance. That is,

$$\int\int_{f^2 \leq \xi^2 + \eta^2 \leq (2f)^2.} |\hat{\mathbf{I}}^2(\xi, \eta)| d\xi d\eta = 2\pi \int_{f^2}^{4f^2} \frac{1}{f^2} df^2 = \text{const.}, \quad \forall f.$$

The descriptive model that accounts for such statistical regularity is surprisingly simple. It was showed by Mumford (1995) that a Gaussian Markov random field (GMRF) model below has exactly $1/f$-Fourier amplitude.

$$p_{1/f}(\mathbf{I};\beta) = \frac{1}{Z}\exp\{-\sum_{x,y}\beta|\nabla\mathbf{I}(x,y)|^2\} \tag{8}$$

where $|\nabla\mathbf{I}(x,y)|^2 = (\nabla_x\mathbf{I}(x,y))^2 + (\nabla_y\mathbf{I}(x,y))^2$. ∇_x and ∇_y are the gradients. As the Gibbs energy is of a quadratic form and its matrix is real symmetric circulant, by a spectral analysis (see Priestley, 1981) its eigen-vectors are the Fourier bases and its eigen-values are the spectra.

This simply demonstrates that much celebrated $1/f$-power law is nothing more than a second order moment constraint in the maximum entropy construction,

$$E_p[|\nabla\mathbf{I}(x,y)|^2] = \frac{1}{2\beta} \approx E_f[|\nabla\mathbf{I}(x,y)|^2], \quad \forall\, x,y. \tag{9}$$

This is equivalent to a $1/f$ constraint in the Fourier amplitude. Since $p_{1/f}(\mathbf{I};\beta)$ is a Gaussian model, one can easily draw a random sample $\mathbf{I} \sim p_{1/f}(\mathbf{I};\beta)$. Figure 4.b shows a typical sample image by Mumford (1995). It has very little structure in it!

2. Descriptive model for natural images with scale-invariant histograms

The second important discovery of natural image statistics is the scale-invariance of gradient histograms (Ruderman 1994, Zhu and Mumford, 1996-97). Take a natural image $\mathbf{I}$, and build a pyramid with a number of n scales, $\mathbf{I} = \mathbf{I}^{(0)}, \mathbf{I}^{(1)}, ..., \mathbf{I}^{(n)}$. $\mathbf{I}^{(s+1)}$ is obtained by an average of 2×2 pixels in $\mathbf{I}^{(s)}$. The histograms $\mathbf{h}^{(s)}$ of gradients $\nabla_x\mathbf{I}^{(s)}(x,y)$ (or $\nabla_y\mathbf{I}^{(s)}(x,y)$) are plotted in Figure 5.a for three scales $s = 0, 1, 2$. Figure 5.b shows the logarithm of the histograms averaged over a number of images.

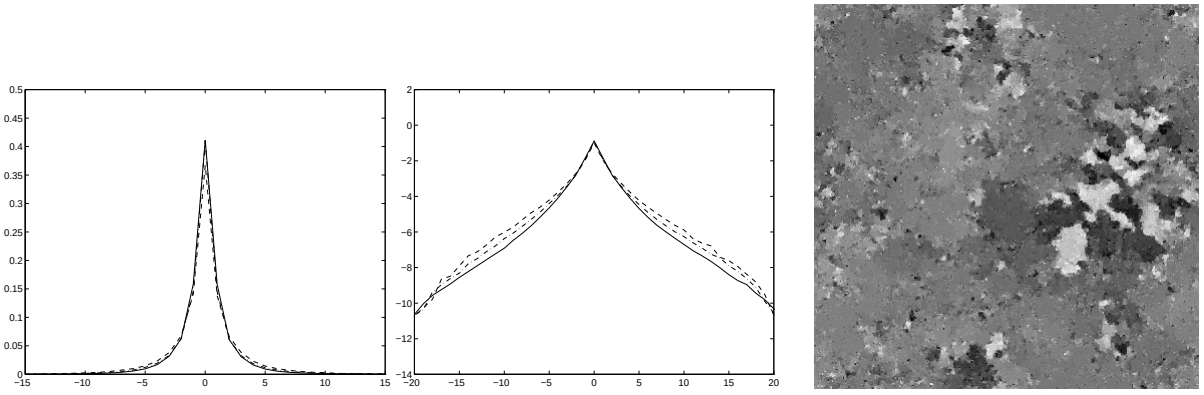

a b c

Figure 5: a). Gradient histograms over three scales. b). Logarithm of histograms. c). A randomly sampled images from a descriptive model $p_{\text{inv}}(\mathbf{I};\boldsymbol{\beta})$. Courtesy of (Zhu and Mumford, 1996-97)

These histograms demonstrate high kurtosis and is amazingly consistent over scales. Let $\mathbf{h}^{\text{obs}}$ be the normalized histogram averaged over 3 scales, and impose constraints that a model p should

produce the same histograms (marginal distributions),

$$E_p[h(\nabla_x \mathbf{I}^{(s)})] = E_p[h(\nabla_y \mathbf{I}^{(s)})] = \mathbf{h}^{\text{obs}}, \quad s = 0, 1, 2, 3, \tag{10}$$

Zhu and Mumford (1996-97) derived a descriptive model,

$$p_{\text{inv}}(\mathbf{I}; \boldsymbol{\beta}) = \frac{1}{Z} \exp\{-\sum_{s=0}^{3} \sum_{(x,y)\in\Lambda^{(s)}} \lambda_x^{(s)}(\nabla_x \mathbf{I}^{(s)}(x,y)) + \lambda_y^{(s)}(\nabla_y \mathbf{I}^{(s)}(x,y))\}. \tag{11}$$

$\Lambda^{(s)}$ is the image lattice at scale s. $\boldsymbol{\beta} = (\lambda_x^{(0)}(), \lambda_y^{(0)}(), ..., \lambda_x^{(3)}(), \lambda_y^{(3)}())$ are the parameters and each $\lambda_x^{(s)}()$ is a 1D potential function quantized by a vector.

Figure 5.c shows a typical image sampled from this model by Gibbs sampler (Geman and Geman, 1984). This image has the scale-invariant histograms shown in Figure 5.a-b. Clearly the sampled image demonstrates some piecewise smoothness and consists of micro-structures of various sizes.

To make connection with other models, we remark on two aspects of $p_{\text{inv}}(\mathbf{I}; \boldsymbol{\beta})$.

Firstly, by choosing only one scale $s = 0$, the constraints in equation (10) is a superset of the constraints in equation (9), as the histogram includes the variance. Therefore p_{inv} also observes the $1/f$-power law.

Secondly, with only one scale, p_{inv} reduces to the general smoothness models widely used in shape-from-X and denoising (see research stream 4). The learned potential functions $\lambda_x()$ and $\lambda_y()$ match pretty close to the manually selected energy functions.

3. Descriptive model for textures

The third descriptive model accounts for interesting psychophysical observations in texture study that histograms of a set of Gabor filters may be *sufficient statistics* in texture perception, i.e, two textures cannot be told apart in early vision if they share the same histograms of Gabor filters (Chubb and Landy, 1991).

Let $F_1, ..., F_K$ be a set of linear filters (such as Laplacian of Gaussian, Gabors), and $h(F_k * \mathbf{I})$ the histograms of filtered image $F_k * \mathbf{I}$ for $k = 1, 2, ..., K$. Each F_k corresponds to an axis and $h(F_k * \mathbf{I})$ a 1D marginal distribution in Fig.3. From an observed image, a set of histograms $\mathbf{h}_k^{\text{obs}}, k = 1, 2, ..., K$ are extracted. By imposing the descriptive constraints

$$E_p[h(F_k * \mathbf{I})] = \mathbf{h}_k^{\text{obs}}, \quad \forall k = 1, 2, ..., K. \tag{12}$$

A FRAME model (Zhu, Wu, and Mumford, 1997-98) is obtained through maximum entropy.

$$p_{\text{tex}}(\mathbf{I}; \boldsymbol{\beta}) = \frac{1}{Z} \exp\{-\sum_{(x,y)\in\Lambda} \sum_{k=1}^{K} \lambda_k(F_k * \mathbf{I}(x,y))\}. \tag{13}$$

where $\boldsymbol{\beta} = (\lambda_1(), \lambda_2(), ..., \lambda_K())$ are potential functions with each function $\lambda_i()$ being approximated by a vector. $p_{\text{tex}}(\mathbf{I}; \boldsymbol{\beta})$ extends traditional Markov random field models (Besag, 1973, Cross and

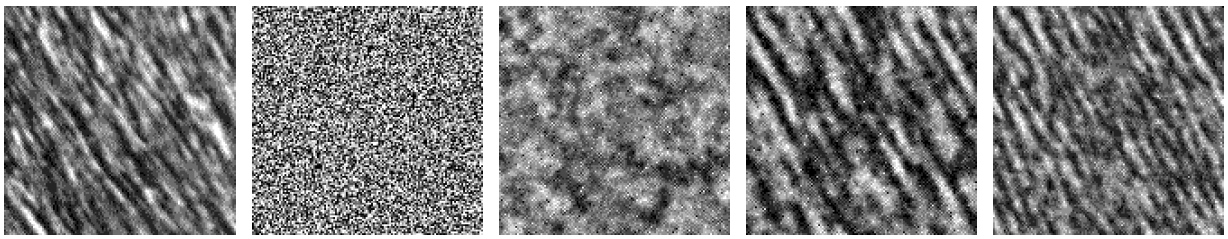

a. observed b. $K = 0$ c, $K = 1$ d. $K = 2$ e. $K = 7$

Figure 6: Learning a sequence of descriptive models for a fur texture: a). The observed texture image, b),c),d),e), are the synthesized images as random samples from $p_{\text{tex}}(\mathbf{I}; \boldsymbol{\beta})$ using $K = 0, 1, 2, 7$ filter histograms respectively. The images are obtained by Gibbs sampler. Courtesy of (Zhu, Wu, and Mumford, 1997)

Jain, 1983) by replacing pairwise cliques with Gabor filters and by upgrading the quadratic energy to non-parametric potential functions which account for high order statistics.

Figure 6 illustrates the modeling of a texture pattern. It uses only one (homogeneous) input image in figure 6.a to estimate the histograms $\mathbf{h}_k^{\text{obs}}, k = 1, 2, ..., K$. With $K = 0$ constraints, $p_{\text{tex}}(\mathbf{I}; \Theta)$ is a uniform distribution and a *typical* random sample is a noise image shown in Figure 6.b. With $K = 1, 2, 7$ histogram constraints, the randomly sampled images from the learned Gibbs models $p_{\text{tex}}(\mathbf{I}; \Theta)$ are shown in figures (6.c,d.e) respectively. The samples are drawn by Gibbs sampler[32] from $p_{\text{tex}}(\mathbf{I}; \boldsymbol{\beta})$ and the selection of filters are governed by a minimax entropy principle[88]. A wide variety of textures are modeled in this way. In a similar way, one can put other statistics in the model (Portilla and Simoncelli, 2000).

4. Descriptive model for texton (attributed point) process

The descriptive models $p_{1/\text{f}}$, p_{inv}, and p_{tex} are all based on lattice and pixel intensities. Now we review a fourth model for texton (attributed point process) which extends lattices to graphs and extends pixel intensity to attributes. Texton processes are very important in perceptual organization. For example, Figure 1 shows a point process for the music band, and Figure 7.a shows a wood pattern where a texton represents a segment of the tree trunk.

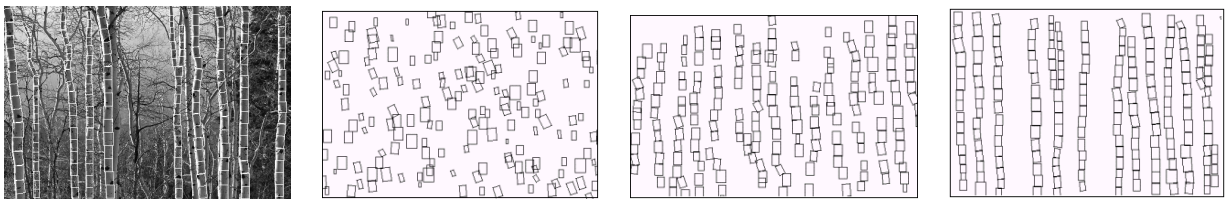

a). observed b). $t = 1$ c). $t = 30$ d). $t = 332$

Figure 7: Different stages of simulating a wood pattern with local spatial interactions of textons. Each texton is represented by a small rectangle. After (Guo, Zhu, and Wu, 2001)

Suppose a texton t has attributes x, y, σ, θ, c for its location, scale, orientation, and photometric

contrast respectively. A texton pattern with an unknown number of n textons is represented by,

$$\mathbf{T} = (n, \{\ t_j = (x_j, y_j, s_j, \theta_j, c_j), j = 1, ..., n\ \}).$$

Each texton t has a neighborhood ∂t defined by spatial proximity, good continuity, parallelism or other Gestalt properties. It can be decided deterministically or stochastically. Once a neighborhood graph is decided, one can extract a set of features $\phi_k(t|\partial t), k = 1, 2, ..., K$ at each t measuring some Gestalt properties between t and its neighbors in ∂t. If the point patterns are homogeneous, then through constraints on the histograms, a descriptive model is obtained to capture the spatial organization of textons (Guo et al 2001),

$$p_{\text{txn}}(\mathbf{T}; \beta_o, \boldsymbol{\beta}) = \frac{1}{Z} \exp\{-\boldsymbol{\beta}_o n - \sum_{j=1}^{n} \sum_{k=1}^{K} \lambda_k(\phi_k(t_j|\partial t_j))\}, \tag{14}$$

p_{txn} is distinct from previous descriptive models in two respects: 1). The number of elements varies, thus a death-birth process must be used in simulating the model. 2). Unlike the static lattice, the spatial neighborhood of each element can change dynamically during the simulation.

Figure 7.a shows an example of a wood pattern with $\mathbf{T}$ given, from which a texton model p_{txn} is learned. Figure 7.b-d shows three stages of the MCMC sampling process of p_{txn} at $t = 1, 30, 332$ sweeps respectively. This example demonstrates that global pattern arises through simple local interactions in p_{txn}. More point patterns are referred to (Guo et al. 2001).

5. Descriptive models for 2D open curves: Snake and Elastica

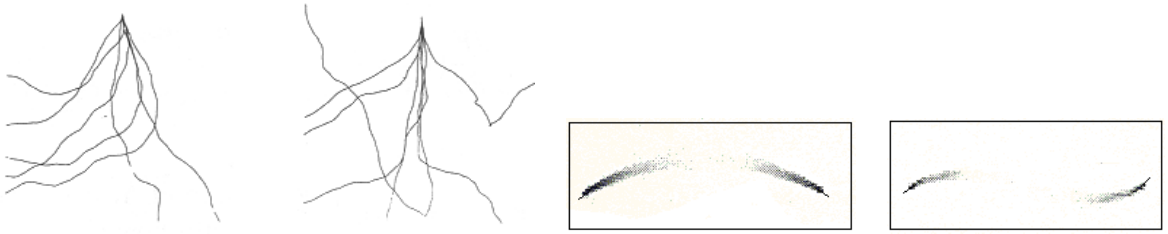

a b c d

Figure 8: a-b). Two sets of random sampled curves from the Elastica model, after (Mumford, 1994), c-d). The stochastic completion fields, After (Williams and Jacobs, 1997).

Moving up the hierarchy from point to curves, we see most curve models are descriptive.

Let $C(s)$ $s \in [a, b]$ be an open curve, there are two curve models in the literature. One is the popular SNAKE or active contour model (Kass etc 1987).

$$p_{\text{snk}}(C; \alpha, \beta) = \frac{1}{Z} \exp\{-\int_a^b \alpha|\nabla C(s)|^2 + \beta|\nabla^2 C(s)|^2 ds\},$$

where $\nabla C(s)$ and $\nabla^2 C(s)$ are the first and second derivatives.

The other is an Elastica model (Mumford, 1994) simulating a Ulenbeck process of a moving particle with friction, let $\kappa(s)$ be the curvature, then

$$p_{\text{els}}(C;\beta) = \frac{1}{Z}\exp\{-\int_a^b [\alpha + \beta\kappa^2(s)]ds\}.$$

α controls the curve length as a decay probability for terminating the curve, like β_o in p_{txn}.

Figures 8.a-b show two sets of randomly sampled curves each starting from an initial point and orientation, the curves show general smoothness like the images in Figure 5.c. Williams and Jacobs (1997) adopted the Elastica model for curve completion. They define the so-called "stochastic completion field" between two oriented line segments (a source and a sink). Suppose a particle is simulated by a random walk, it starts from the source and ends at the sink. The completion fields shown in Figures 8.c-d show the probability that the particle passing a point (x, y) in the lattice (dark means high probability). This was used as a model for illusory contours.

6. Descriptive models for 2D closed curves

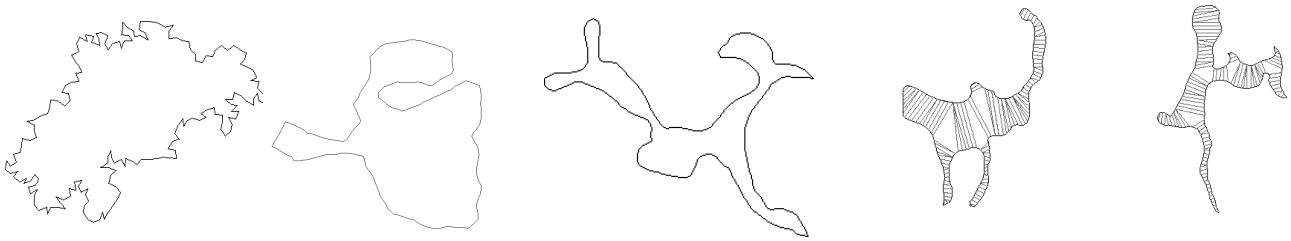

a). $K = 0$ b). $K = 2$ c). $K = 5$ d). $K = 5$ e). $K = 5$

Figure 9: Learning a sequence of models $p_{\text{shp}}(\Gamma;\boldsymbol{\beta})$ for silhouettes of animals and plants, such as cats, dogs, fish, and leaves. a-e are typical samples from p_{shp} with $K = 0, 2, 5, 5, 5$ respectively. The line segments show the medial axis features. Courtesy of (Zhu, 1999)

The next descriptive model generalizes the smoothness curve model to 2D shape models with both contour and region based features. Let $\Gamma(s),\ s \in [0, 1]$ be a simple closed curve of normalized length. One can always represent a curve by polygon with a large enough number of vertices. Some edges can be added on the polygon for spatial proximity, parallelism, and symmetry. Thus a random graph structure is established, and some Gestalt properties $\phi_k(), k = 1, 2, ..., K$ can be extracted at each vertex and its neighbors, such as co-linearity, co-circularity, proximity, parallelism etc. Through constraints on the histograms of such features, a descriptive model is obtained in (Zhu, 1999),

$$p_{\text{shp}}(\Gamma;\boldsymbol{\beta}) = \frac{1}{Z}\exp\{\sum_{k=1}^{K}\int_0^1 \lambda_k(\phi_k(s))ds\}, \tag{15}$$

This model is invariant to translation, rotation and scaling. By choosing features $\phi_k(s)$ to be $\nabla, \nabla^2, \kappa(s)$, this model is a non-parametric extension of the SNAKE and Elastica models on open curves.

Figure 9 shows a sequence of shapes randomly sampled from $p_{\text{shp}}(\Gamma;\boldsymbol{\beta})$. The training ensemble includes contours of animals and tree leaves. The sampled shapes at $K = 0$ (i.e.. no features) are very irregular (sampled by Markov chain random walk under the hard constraint that the curve is closed and has no self-intersection. The MC starts with a circle), and become smooth at $K = 2$ which integrates two features: co-linearity and co-circularity measured by the curvature and derivative of curvature $\kappa(s)$ and $\nabla\kappa(s)$ respectively. Elongated and symmetric "limbs" appear at $K = 5$ when we integrates crossing region proximity, parallelism etc.

7. Descriptive models for 2D human face

Moving up to high level patterns, descriptive models were used for modeling human faces (Yuille, 1991) and hand (Grenander et al. 1991), but early deformable models were manually designed, though in principle, they could be re-formulated in the maximum entropy form. Recently a descriptive face model is learned from data by (Liu etc. 2001) following the minimax entropy scheme.

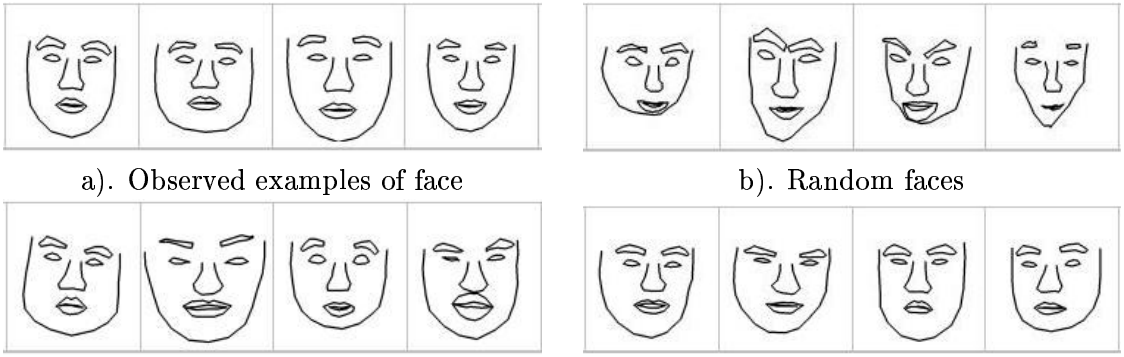

a). Observed examples of face b). Random faces

c) Random faces with 4 features matched d). Random faces with 17 features matched

Figure 10: Learning a sequence of face models $p_{\text{fac}}(V;\boldsymbol{\beta})$. a). Four of the observed faces as training data, b,c,d). Four of the stochastically sampled faces with $K = 0, 4, 17$ statistics respectively. Courtesy of (Liu, Zhu, and Shum, ICCV, 2001)

A face is represented by a list of n (e.g. $n = 83$) key points which are manually decided. Connecting these points forms the sketch shown in Figure 10. Thus each face is a point in a 166-space. After normalization in location, rotation and scaling, it has 162 dimensions. Figure 10.a shows four of example faces from the data ensemble.

Unlike the previous homogeneous descriptive models where all elements in a graph (or lattice) are subject to the same statistical constraints, the key points are labeled, and thus different statistical constraints are imposed at each location.

Suppose we extract K features $\phi_k(V), k = 1, 2, ..., K$ on the graph V, then a descriptive model is,

$$p_{\text{fac}}(V;\boldsymbol{\beta}) = \frac{1}{Z}\exp\{-\sum_{k=1}^{K}\lambda_k(\phi_k(V))\}. \tag{16}$$

Liu etc. did a PCA to reduce the dimension first, and therefore the features $\phi_k(V)$ are extracted

on the PCA co-efficients. Figure 10.b shows four sampled faces from a uniform model in the PCA-coefficient space bounded by the co-variances. The sampled faces in Figures 10.c-d become more pleasant as we increase the number of features. When $K = 17$, the synthesized faces are no longer distinguishable from faces in the observed ensemble.

Summary: a continuous spectrum of models on the space of random graphs

To summarize this section, visual patterns, ranging from generic natural images, textures, textons, curves, shapes, and objects, can all be represented on random graphs. A random graph has a varying number of vertices and edges, and has both attribute variables and address variables. All the descriptive models reviewed in this section are focused on different subspaces of a huge space of random graphs. Thus these models are examples in a "continuous" spectrum in the graph space (see eq.(3))! Though the general ideas of defining probability on random graphs were discussed in Grenander's pattern theory (Grenander, 1976-81), it will be a long way for developing such models as well as discovering a sufficient set of features and statistics on various graphs.

5 Conceptualization of visual patterns and statistics physics

Now we study an important theoretical issue associated with visual modeling: how do we define a visual pattern mathematically? For example, what is the definition of a human face, a tree, or a texture? In mathematics, a concept is equalized to a set. However a visual pattern is characterized by a probabilistic model as the previous section showed. The connection between a deterministic set and a statistical model was established in modern statistical physics through a general theorem dated back to (Gibbs, 1902).

5.1 Background: statistical physics and ensembles

Modern statistical physics is a subject studying macroscopic properties of a system involving massive amount of elements(see Chandler, 1987). Figure 11 illustrates three types of physical systems which are interesting to us.

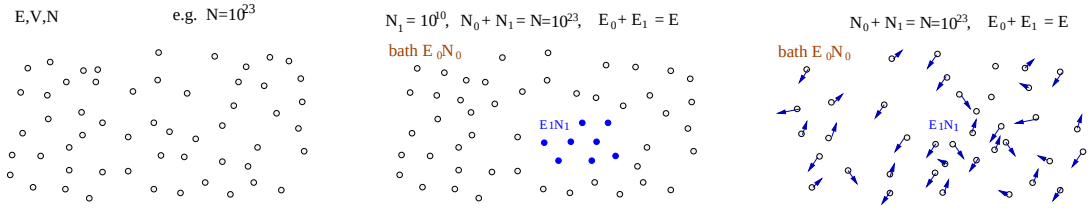

a). micro-canonical ensemble b). canonical ensemble c). grand-canonical ensemble

Figure 11: Three typical ensembles in statistical mechanics.

1. Micro-canonical ensembles. Figure 11.a is an insulated system of N elements. The elements could be atoms, molecules, electrons in systems such as gas, ferro-magnetic material, fluid etc. N is really big, say $N = 10^{23}$ and is considered infinity. The system is decided by a configuration or

state $s = (\mathbf{x}^N, \mathbf{m}^N)$, where $\mathbf{x}^N$ describes the coordinates of the N elements and $\mathbf{m}^N$ their momenta (Chandler, 1987). The system is subject to some global constraints $\mathbf{h}(s) = (N, E, V)$. That is, the number of elements N, the total energy $E(s)$, and total volume V are fixed.

Statistical physics characterizes the above insulated system at thermodynamic equilibrium by a so-called *micro-canonical ensemble*,

$$\Omega_{mce}(\mathbf{h}_o) = \{s = (\mathbf{x}^N, \mathbf{m}^N) : \mathbf{h}(s) = \mathbf{h}_o = (N, V, E)\}.$$

s is a microscopic state or **instance**, and $\mathbf{h}(s)$ is the macroscopic **summary** of the system state. Thus Ω_{mce} is a deterministic set or an equivalence class for all states that satisfy a descriptive constraints $\mathbf{h}(s) = \mathbf{h}_o$.

An essential assumption in statistical physics is,

> *"all microscopic states are equally likely at thermodynamic equilibrium."*

This is simply a maximum entropy assumption. Let $\Omega \ni s$ be the space of all possible states, then $\Omega_{mce} \subset \Omega$ is associated with a uniform probability,

$$p_{\text{unif}}(s; \mathbf{h}_o) = \begin{cases} 1/|\Omega_{mce}(\mathbf{h}_o)| & \text{for } s \in \Omega_{mce}(\mathbf{h}_o), \\ 0 & \text{for } s \in \Omega / \Omega_{mce}(\mathbf{h}_o). \end{cases}$$

2. Canonical ensembles. The canonical ensemble refers to a small system (with fixed volume V_1 and elements N_1) embedded in a micro-canonical ensemble, see Figure 11.b. The canonical ensemble can exchange energy with the rest system (called heat bath or reservoir). The system is relatively so small, e.g $N_1 = 10^{10}$ that the bath can be considered a micro-canonical ensemble.

At thermodynamic equilibrium, the microscopic state s_1 for the small system is governed by a Gibbs distribution,

$$p_{\text{Gib}}(s_1; \boldsymbol{\beta}) = \frac{1}{Z} \exp\{-\boldsymbol{\beta} E(s_1)\}$$

The conclusion was stated as a general theorem by Gibbs (1902),

> *"If a system of a great number of degrees of freedom is micro-canonically distributed in phase, any very small part of it may be regarded as canonically distributed."*

Basically this theorem states that the Gibbs model p_{Gib} is a conditional probability of the uniform model p_{unif}, and thus it bridges a deterministic set Ω_{mce} with a descriptive model p_{Gib}. Some detailed deduction of this conclusion in vision models can be found in (Wu and Zhu, 1999).

3. Grand-Canonical ensembles. When the small system with fixed volume V_1 can also exchange elements with the bath as in liquid and gas materials, then it is called a grand-canonical ensemble, see Figure 11.c. The grand-canonical ensemble follows a distribution,

$$p_{\text{gce}}(s_1; \beta_o, \beta) = \frac{1}{Z} \exp\{-\beta_o N_1 - \beta E(s_1)\},$$

where an extra parameter β_o controls the number of elements N_1 in the ensemble.

5.2 Conceptualization of visual patterns

The connections between the three physical ensembles reveals an important duality between a *descriptive constraints* $\mathbf{h}(s) = \mathbf{h}_o$ in the deterministic set $\Omega_{\text{mcn}}(\mathbf{h}_o)$ and the parameters $\boldsymbol{\beta}$ in Gibbs model p_{Gib}. In vision, the duality is between the image statistics $\mathbf{h}_o = (\mathbf{h}_1^{\text{obs}}, ..., \mathbf{h}_K^{\text{obs}})$ in equation (6) and the parameters of the descriptive models $\boldsymbol{\beta} = (\lambda_1, ..., \lambda_K)$. Thus a visual pattern can be readily defined based on this setting.

In the literature, a texture pattern was first defined as a Julesz ensemble by (Zhu et al. 1999-2000). This can be easily extended to any patterns, including, generic images, texture, smooth surfaces, texton process, etc.

Definition 2 *:* **(homogeneous visual patterns)**. *For any homogeneous visual pattern v defined on a lattice or graph Λ, let s be the visual representation (e.g. $s = \mathbf{I}$) and $\mathbf{h}(s)$ a list of sufficient feature statistics, then a pattern v is equal to a maximum set (or equivalence class), as Λ goes to infinity in the von Hove sense,*

$$\text{A pattern } \; v = \Omega(\mathbf{h}_o) = \{s_\Lambda : \; \mathbf{h}(s) = \mathbf{h}_o, \; \Lambda \to \infty\}. \tag{17}$$

As Λ goes to infinity and the pattern is homogeneous, the statistical fluctuations and the boundary condition effects both diminish. Thus the normalized statistics $\mathbf{h}(s)$ converges to a value $\mathbf{h}_o$.

Any visual pattern is defined for a purpose. The purpose is reflected in the selection of "sufficient" statistics $\mathbf{h}(s)$. That is, depending on a visual task, we are only interested in some global (macro) properties $\mathbf{h}(s)$, and we are not interested in the differences between instances within the set. Similarly in statistical physics, one is only concerned with macroscopic properties, such as, temperature, pressure, energy etc. In vision, such macroscopic property $\mathbf{h}$ corresponds best to the Gestalt concept "whole".

The connection between set $\Omega(\mathbf{h}_o)$ and the descriptive model $p(s; \boldsymbol{\beta})$ is re-stated informally by the theorem below (Wu and Zhu, 1999).

Theorem 3 (Ensemble equivalence). *For visual signals $s_\Lambda \in \Omega(\mathbf{h}_o)$ on large (or infinity) lattice (or graph) Λ, then on any small lattice $\Lambda_o \subset \Lambda$, the signal s_{Λ_o} given its neighborhood $s_{\partial\Lambda_o}$ is subject to a descriptive model $p(s_{\Lambda_o}|s_{\partial\Lambda_o}; \boldsymbol{\beta}_o)$.*

The duality between $\boldsymbol{\beta}_o$ and $\mathbf{h}_o$ is reflected by the maximum entropy constraints $E_{p(s;\boldsymbol{\beta}_o)}[\mathbf{h}(s)] = \mathbf{h}_o$. More precisely, it is stated in the following theorem (Wu and Zhu, 1999).

Theorem 4 (Model and concept duality). *Let $p(s_\Lambda; \boldsymbol{\beta})$ be a descriptive model of a pattern v, and $\Omega_\Lambda(\mathbf{h})$ the set for pattern v, and let $\psi(\mathbf{h})$ and $\rho(\boldsymbol{\beta})$ be the entropy function and pressure defined as*

$$\psi(\mathbf{h}) = \lim_{\Lambda\to\infty} \frac{1}{|\Lambda|} \log |\Omega_\Lambda(\mathbf{h})|, \quad \text{and} \quad \rho(\boldsymbol{\beta}) = \lim_{\Lambda\to\infty} \frac{1}{|\Lambda|} \log Z(\boldsymbol{\beta}).$$

If $\mathbf{h}_o$ *and* $\boldsymbol{\beta}_o$ *correspond to each other, then*

$$\phi'(\mathbf{h}_o) = \boldsymbol{\beta}_o, \quad \text{and} \quad \rho'(\boldsymbol{\beta}_o) = \mathbf{h}_o,$$

in the absence of phase transition.

For visual patterns which are inhomogeneous or defined on finite graphs, such as a human face or a 2D shape of animal, the definition of pattern is given below.

Definition 3 (Inhomogeneous finite patterns). *For inhomogeneous visual pattern* v *defined on a finite lattice or graph* Λ*, let* s *be the representation, and* $\mathbf{h}(s)$ *its sufficient statistics, the visual concept is an ensemble governed by a maximum entropy probability* $p(s; \boldsymbol{\beta})$*,*

$$\text{pattern } \mathrm{v} = \Omega(\mathbf{h}_o) = \{(s,\ p(s : \boldsymbol{\beta})) :\ E_p[\mathbf{h}(s)] = \mathbf{h}_o\}. \tag{18}$$

Each pattern instance s *is associated with a probability* $p(s; \boldsymbol{\beta})$*.*

Obviously, the definition in equation (17) is a special case of equation (18). That is, when $\Lambda \to \infty$, one homogeneous signal is enough to compute the expectation, i.e. $E_p[\mathbf{h}(s)] = \mathbf{h}(s)$. The limit of $p(s; \boldsymbol{\beta})$ is the uniform probability $p_{\text{unif}}(s; \mathbf{h}_o)$ as $\Lambda \to \infty$.

The probabilistic notion in defining finite visual signal is the root for errors in recognition, segmentation, and grouping. An in-depth discussion on the relationship between an error bound and models are referred to the order parameter theory (Yuille, Coughlan, Wu, and Zhu, 2001).

6 Generative modeling

So far, we have reviewed the theory, examples and conceptualization using descriptive models, Two important questions remain unanswered. 1). How do we discover the visual representation beyond raw pixels, such as curves, shape, and faces? 2). How do we assemble the spectrum of visual patterns into a generic model of natural images? In this section, we review progress in generative modeling, which provides a way for answering these questions.

6.1 The basic principle of generative modeling

Now we return to the general learning problem in Section (3). Generative models approach $f(\mathbf{I})$ by a sequence of probability models that engage hidden (latent) variables for the underlying structures. For example, one may assume that a scene consists of a number of objects, each object has a number of parts and surfaces, each surface has a boundary and 3D geometric shape, there are textures, colors and marks painted on surface, under a certain lighting condition, an image $\mathbf{I}$ is generated.

For simplicity of notation, we assume L-levels of hidden variables which generate image $\mathbf{I}$ in a linear order,

$$W_L \xrightarrow{\mathcal{D}_L} W_{L-1} \xrightarrow{\mathcal{D}_{L-1}} \cdots \xrightarrow{\mathcal{D}_2} W_1 \xrightarrow{\mathcal{D}_1} \mathbf{I}. \tag{19}$$

At each level, W_i generates W_{i-1} with a dictionary (vocabulary) $\mathcal{D}_i, i = 1, ..., L$. The dictionary is a set of description, such as image bases, textons, parts, templates, lighting functions etc.

Let $p(W_{i-1}|W_i; \mathcal{D}_i, \boldsymbol{\beta}_{i-1})$ denote the conditional distribution for pattern W_{i-1} given W_i, with $\boldsymbol{\beta}_{i-1}$ being the parameter of the model. Then by summing over the hidden variables, we have an image model,

$$p(\mathbf{I}; \Theta) = \sum_{W_L} \cdots \sum_{W_1} p(\mathbf{I}|W_1; \mathcal{D}_1, \boldsymbol{\beta}_0) p(W_1|W_2; \mathcal{D}_1, \boldsymbol{\beta}_1) \cdots p(W_{L-1}|W_L; \mathcal{D}_L, \boldsymbol{\beta}_{L-1}). \tag{20}$$

$\Theta = (\mathcal{D}_1, ..., \mathcal{D}_L; \boldsymbol{\beta}_0, ..., \boldsymbol{\beta}_{L-1})$ are the parameters, and each conditional probability is a descriptive model.

By analogy to speech, the observable signal $\mathbf{I}$ is the speech wave form. Then the first level dictionary $\mathcal{D}_1$ is the set of *phonemes*, and $\boldsymbol{\beta}_1$ parameterizes the transition probability between phonemes. The second level dictionary $\mathcal{D}_2$ is the set of *words*, each being a short sequences of phonemes in $\mathcal{D}_1$, and $\boldsymbol{\beta}_2$ parameterizes the transition probability between words. Going up the hierarchy, we need dictionaries of *grammatic reproduction rules* for phrases and sentences, and probabilities for how frequently each reproduction rule is used, and so on.

The hidden variables W_i is fundamentally different from the image features ϕ_i in descriptive models, though they may be closely related (see section (9)). W_i are *random variables* that should be inferred from images, while ϕ_i are *deterministic transforms* of images.

The reasons for engaging hidden variables are two-fold. Firstly, for certain vision tasks, such as navigation, grasping objects, we need such high level descriptions. Secondly, as it is said in the desk example before, the variables in W_i are less dependent of each other conditioned on W_{i+1}. Thus the model $p(W_i|W_{i+1}; \mathcal{D}_{i+1}, \boldsymbol{\beta}_i)$ is much easier to learn than the model $p(W_i; \boldsymbol{\beta}_i)$.

Following the ML-estimate in equation(2), we can learn the parameters Θ in $p(\mathbf{I}; \Theta)$ by EM-type algorithm, like stochastic gradients (Gu and Kong, 1998). By taking the derivative of the log-likelihood with respect to Θ, i.e setting $\frac{d\partial \log p(\mathbf{I};\Theta)}{d\Theta} = 0$. We have

$$\begin{aligned} 0 = \sum_{W_L} \cdots \sum_{W_1} \quad & [\frac{\partial \log p(\mathbf{I}|W_1; \mathcal{D}_1, \boldsymbol{\beta}_0)}{\partial(\mathcal{D}_1, \boldsymbol{\beta}_0)} + \cdots + \frac{\partial \log p(W_{L-1}|W_L; \mathcal{D}_L, \boldsymbol{\beta}_{L-1})}{\partial(\mathcal{D}_L, \boldsymbol{\beta}_{L-1})}] \\ & \times p(W_1|\mathbf{I}; \mathcal{D}_1, \boldsymbol{\beta}_0) \cdots p(W_L|W_{L-1}; \mathcal{D}_L, \boldsymbol{\beta}_{L-1}) \end{aligned} \tag{21}$$

This huge equation can be solved with global optimal by iterating two steps (Gu and Kong, 1998):

1. The E-type step: making inferences about the hidden variables by sampling from a sequence of posteriors,

$$W1 \sim p(W_1|\mathbf{I}; \mathcal{D}_1, \boldsymbol{\beta}_0), \quad \cdots, \quad W_L \sim p(W_L|W_{L-1}; \mathcal{D}_L, \boldsymbol{\beta}_{L-1}). \tag{22}$$

Then we can approximate the summation (integration) by importance sampling. We should discuss the effective sampling using discriminative models in Section (9.2).

2. The M-type step: optimizing the parameters Θ. The learning results in Θ includes a hierarchic visual dictionary $\mathcal{D}_1, ..., \mathcal{D}_L$ and the descriptive models $\boldsymbol{\beta}_0, ..., \boldsymbol{\beta}_{L-1}$ that govern their spatial layouts of the hidden structures. It is beyond this review to discuss the algorithm.

6.2 Some examples of generative models

Now we review a spectrum of generative models, starting with the models for the $1/f$.

1. A generative model for the $1/f$-power law

The $1/f$-law of the Fourier amplitude in natural images was analytically modeled by a Gaussian MRF $p_{1/\mathrm{f}}$ (Mumford, 1995). We transform equation (8) into the Fourier domain, thus

$$p_{1/\mathrm{f}}(\mathbf{I};\beta) = \frac{1}{Z}\exp\{-\sum_{\xi,\eta}\beta(\xi^2+\eta^2)|\hat{\mathbf{I}}(\xi,\eta)|^2\}. \tag{23}$$

The Fourier bases are the independent components for the Gaussian ensemble governed by $p_{1/\mathrm{f}}$. From the above Gaussian model, one obtains a two-layer generative model (Mumford, 1995),

$$\mathbf{I}(x,y) = \sum_{\xi}\sum_{\eta}\frac{1}{2\beta(\xi^2+\eta^2)}a(\xi,\eta)e^{2\pi i\frac{x\xi+y\eta}{N}}, \quad a(\xi,\eta)\sim N(0,1). \tag{24}$$

The dictionary $\mathcal{D}_1$ is the Fourier basis, the parameters are $(0,1)$ for the normal density, and the hidden variables are the Fourier coefficients $a(\xi,\eta)\ \forall\xi,\eta$ which are iid normal distributed, therefore,

$$\mathcal{D}_1 = \{\ \mathbf{b}(\mathbf{I};\xi,\eta) = e^{2\pi i\frac{x\xi+y\eta}{N}} : \forall\xi,\eta\ \} \quad \boldsymbol{\beta} = (0,1), \quad \text{and} \quad W_1 = \{a(\xi,\eta):\forall\xi,\eta\}.$$

One can sample a random image $\mathbf{I}\sim p_{1/\mathrm{f}}(\mathbf{I};\beta)$ according to equation (24): 1). drawing the iid Fourier coefficients, 2). generating the synthesis image $\mathbf{I}$ by linear superposition of the Fourier bases. A result is displayed in Figure 4.b.

To our knowledge, this is the only image model whose descriptive and generative versions are analytically transferable. Such happy endings perhaps only occur in Gaussian models.

In the literature, (Ruderman, 1997) explains the $1/f$-law by an occlusion model. It assumes that image $\mathbf{I}$ is generated by a number of independent "objects" (rectangles) of size subject to a cubic law $1/r^3$. A synthesis image is shown in Figure 12.a.

2. A generative model for scale-invariant gradient histograms

The scale-invariance of gradient histograms in natural images. inspired a number of research for generative models as well in parallel with the descriptive models p_{inv}. The objective is to search for some "laws" that governs the distribution of objects in natural scenes.

One is the random collage model (Lee et al. 2000), which is also called a dead leaves model (see Stoyan et al 1985). It assumes that an image is generated by a number of n opaque disks. Each disk is represented by hidden variables x, y, r, α for center, radius, and intensity respectively.

$$W_1 = (n, \{x_i, y_i, r_i, \alpha_i) : i = 1, 2, ..., n\}), \quad \mathcal{D}_1 = \{disk(\mathbf{I}; x, y, r) : \forall (x, y) \in \Lambda, r \in [r_{\min}, r_{\max}].\}$$

The dictionary $\mathcal{D}_1$ includes disk templates at all possible sizes and locations. Lee et al.(2000) showed that if $p(n)$ is Poisson distributed, and the disk location (x, y) and intensity α are iid uniform distributed, and the radius r_i subject to a $1/r^3$-law,

$$p(r) = c/r^3, \quad \text{for } r \in [r_{\min}, r_{\max}] \tag{25}$$

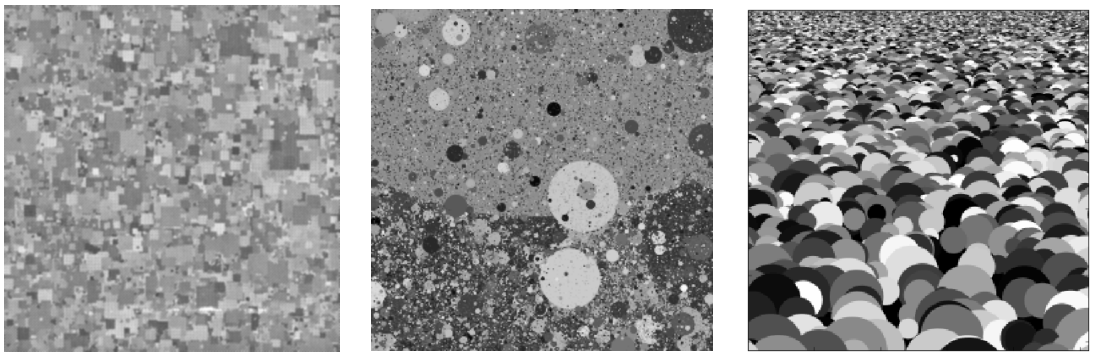

a b c

Figure 12: Synthesized images from three generative models. a). Ruderman, 1997. b) Lee et al 2000, c). Chi and Geman, 1998. See text for explanations.

Then the generative model $p(\mathbf{I};\Theta)$ has scale invariance gradient histograms. Figure 12.b shows a typical image sampled from this model.

The second model is studied by Chi and S.Geman (1998). This offers a beautiful 3D generative explanation. It assumes that the disks (objects) are sitting vertically on a 2D plane (the ground) facing the viewer. The sizes of the disks are iid uniformly distributed, and Chi proved that the 2D projected (by perspective projection) sizes of the objects then follow the $1/r^3$ law in equation (25). The locations and intensities are iid uniformly distributed like the random collage model. A typical image sampled from this model is shown in Figure 12.c. More rigorous studies and laws along this vein are in (Mumford and Gidas, 2001). These results put a reasonable explanation for the origin of scale invariance in natural images. Nevertheless these models are all biased by the object elements they choose, i.e. they are not maximum entropy models.

3. Generative model for sparse coding: learn the dictionary

In research stream 2 (image coding, wavelets, image pyramids, ICA etc) discussed in section (2.1), a linear additive model is widely assumed and an image is a superposition of some local image bases from a dictionary plus a Gaussian noise image $\mathbf{n}$.

$$\mathbf{I} = \sum_{i}^{n} \alpha_i \cdot \psi_{\ell_i, x_i, y_i, \tau_i, \sigma_i} + \mathbf{n}, \qquad \psi_i \in \mathcal{D},\ \forall i. \tag{26}$$

A base is indexed by $b_i = (\ell_i, \alpha_i, x_i, y_i, \tau_i, \sigma_i)$ for its type of base function, coefficient, center, orientation, and scale. Thus we have a two-layer generative model,

$$W_1 = (n, \{b_i : i = 1, 2, ..., n\};\ \mathbf{n}), \quad \mathcal{D}_1 = \{\psi_\ell(x, y, \tau, \sigma) : \forall x, y, \tau, \sigma, \ell.\}$$

ψ_ℓ is a base function, for example, Gabor, Laplacian of Gaussian etc. The hidden variables $x_i, y_i, \tau_i, \sigma_i$ are assumed iid uniformly distributed, and the coefficients $\alpha_i \sim p(\alpha),\ \forall i$. For example

$p(\alpha)$ is a Laplacian or mixture of Gaussian for sparse coding,

$$p(\alpha) \sim \exp\{-|\alpha|/c\} \quad \text{or} \quad p(\alpha) = \sum_{j=1}^{2} \omega_j N(\alpha, \sigma_j). \tag{27}$$

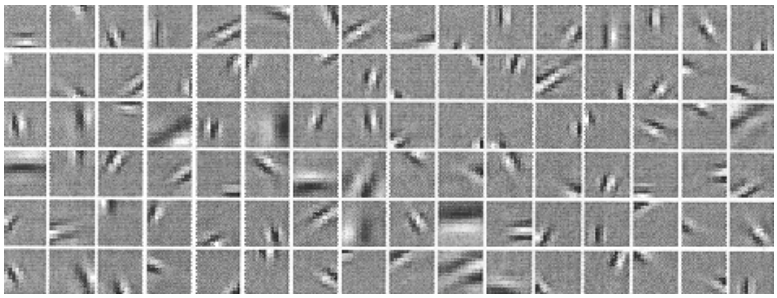

Figure 13: Some of the linear bases (dictionary) learned from natural images by (Olshausen and Field,1997)

According to the theory of generative model (section (6.1)), one can learn the dictionary from raw images in the M-step. Olshausen and Field (1995-97) used the sparse coding prior $p(\alpha)$ learned a set of $144 = 12 \times 12$ pixels bases, some of which are shown in Figure 13. Such bases capture some image structures and are believed to bear resemblance to the responses of simple cells in V1 of primates.

4. A generative model for texton and texture: model integration

In the previous three generative models, the hidden variables are assumed to be iid distributed. Such distributions are degenerated descriptive models. But obviously these variables and objects are not iid, and sophisticated descriptive models are needed for the spatial relationships between the image bases or objects.

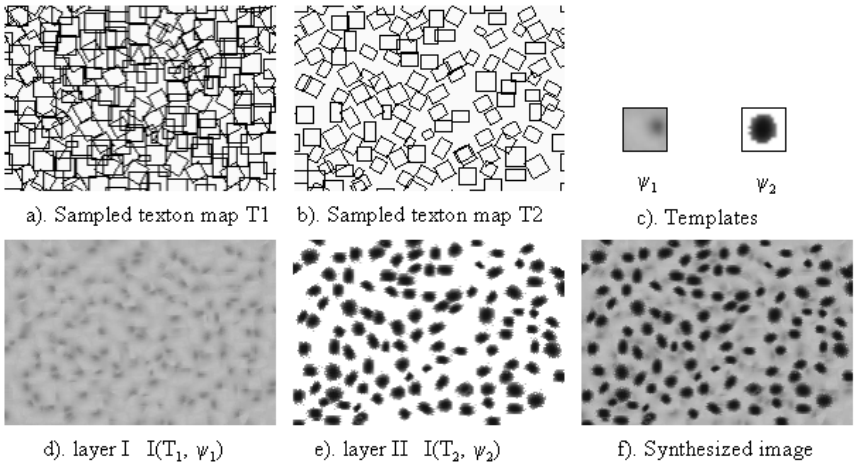

Figure 14: An example of integrating descriptive texton model and a generative model for a cheetah skin pattern. After (Guo et al 2001).

The first work that integrates the descriptive and generative model was presented by (Guo et al. 2001) for texture modeling. It assumes that a texture image is generated by two levels

(foreground and background) of hidden texton processes plus a Gaussian noise. Figure 14 shows an example of cheetah skin pattern. Figure 14.a-b shows two texton patterns $\mathbf{T}_1, \mathbf{T}_2$, which are sampled from descriptive textons models $p_{\text{txn}}(\mathbf{T}; \boldsymbol{\beta}_{o,1}, \boldsymbol{\beta}_1)$ and $p_{\text{txn}}(\mathbf{T}; \boldsymbol{\beta}_{o,2}, \boldsymbol{\beta}_2)$ respectively. The models are learned from an observed cheetah skin (raw pixel) image. Each texton is symbolically illustrated by an oriented window. Then two base functions ψ_1, ψ_2 are learned from images and shown in Figure 14.c. The two image layers are shown in Figure 14.d-e. The superposition (with occlusion) of the two layers renders the synthesized image in Figure 14.f. More examples and discussions are referred to (Guo, et al ICCV 2001).

5. A generative rope model of curve processes

Now we show a two-layer generative model for curve processes. This is called a "rope model" by (Tu and Zhu, ECCV 2002). The model extends the descriptive model for SNAKE and Elastica p_{snk} and p_{els} by integrating it with base representation.

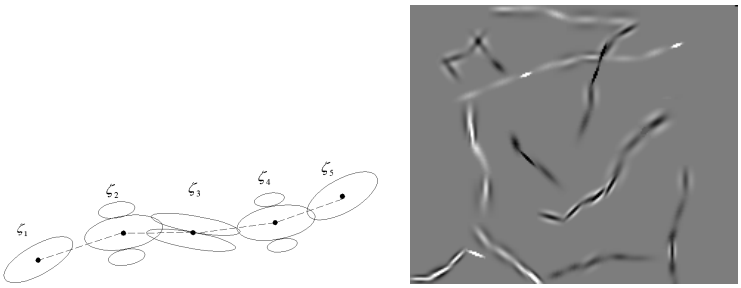

a b

Figure 15: a). A rope model is a Markov chain of knots and each knot has 1-3 image bases shown by the ellipses. b). Random ropes sampled from the prior model $p(C)$. After (Tu and Zhu, ECCV 2002)

Figure 15.a shows a sketch of the rope model C which is a Markov chain of knots. Each knot ζ has 1-3 linear bases, for example, Gaussians, difference of Gaussian (DoG), and difference of offset Gaussians (DOOG) at various orientations and scales

$$W = (n, \zeta_1, \zeta_2, ..., \zeta_n), \quad \text{with} \quad \zeta_i = (\alpha_{ij}, \ell_{ij}, x_{ij}, y_{ij}, \tau_{ij}, \sigma_{ij})_{j=1}^{k}, \ k \leq 3.$$

Figure 15.b shows a number of random curves (image not pure geometry) sampled from the rope model. In summary, the rope model groups image bases into curves and thus extends the previous iid image coding model.

Summary The generative models used in vision are still very preliminary, and they often assume a degenerated descriptive model for the hidden variables. The effective integration of generative and descriptive models is the major direction for visual modeling.

7 Conceptualization of patterns and their parts: revisited

With generative models, we now revisit the conceptualization of visual patterns in a more general setting.

In Section (5.2), a visual pattern v with representation s is equalized to a statistical ensemble governed by a descriptive model $p(s;\boldsymbol{\beta})$. Mathematically the concept v is identified by a number $\boldsymbol{\beta}$ (or its duality $\mathbf{h}$) in a descriptive probability family Ω_K^d (see expression (3) for notation).

$$\text{A visual pattern v} \longleftrightarrow \mathbf{h} \longleftrightarrow \boldsymbol{\beta} \in \Omega_K^d.$$

In reality, the representation s is only our inner perception, and is not observable unless s is an image. Thus we need to define visual concepts based on images so that they can be learned and verified from observable data.

Following the notation is Section (6.1), we have the following definition extending from definition 3.

Definition 4 (visual pattern) *A visual pattern v is a statistical ensemble of image $\mathbf{I}$ governed by a generative model $p(\mathbf{I};\Theta)$ with L layers,*

$$\text{pattern v} = \Omega(\Theta^v) = \{\ (\mathbf{I}, p(\mathbf{I};\Theta^v))\ \},$$

where $p(\mathbf{I};\Theta^v))$ is defined in equation (20).

In this definition, a pattern v is identified by a vector of parameters in the generative family Ω_K^g, which include the L dictionaries and L descriptive models,

$$\text{A visual pattern v} \longleftrightarrow \Theta^v = (\mathcal{D}_1^v, ..., \mathcal{D}_L^v, \boldsymbol{\beta}_0^v, ..., \boldsymbol{\beta}_{L-1}^v) \in \Omega_K^g$$

The definition includes many ensemble of visual patterns for its hidden variables which are governed by the descriptive models in $p(\mathbf{I};\Theta)$. By analogy to speech, Θ^v defines the whole language system, say $v = \textit{English}$ or $v = \textit{chinese}$, and it includes all the hierarchic descriptions from waveforms to phonemes, and to sentences – both the vocabulary and models. Therefore, it is clear that the definition of many intuitive but vague concepts, such as textons, meaningful parts of shape etc, are defined in the context of a generative model Θ.

Definition 5 (visual vocabulary) *A visual vocabulary, such as textons, meaningful parts of shape etc. are defined as an element in the dictionaries $\mathcal{D}_i, i = 1, ..., L$ associated with the generative model of natural images $p(\mathbf{I};\Theta)$.*

To show some recent progress, we show a three-level generative model for texture. It assumes that a texture image $\mathbf{I}$ is generated by a linear superposition of bases W_1 in equation (27). These bases are generated by a smaller number of textons W_2. Each textons is a deformable template consists of a few bases.

$$\text{textons } W_2 \xrightarrow{\mathcal{D}_2} \text{bases} \xrightarrow{\mathcal{D}_1} \mathbf{I}$$

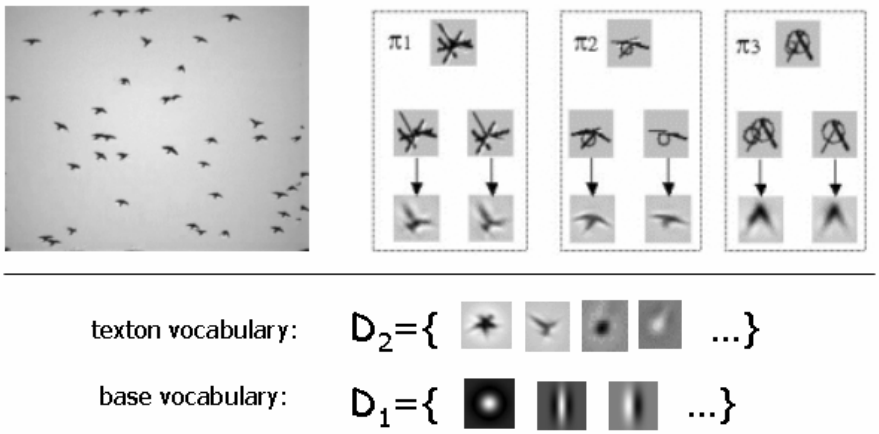

Figure 16: Learning textons from images. After (Zhu, et al. ECCV 2002).

Figure 16 shows a recent work by Zhu et al (2002) for learning the texton representation from texture images. The vocabulary $\mathcal{D}_1$ is three bases (Gabor sine, Gabor Cosine, and Laplacian of Gaussian) at various orientations and scales. Given a bird image, three typical texton template are learned and shown on the right side of figure 16. Each texton template (π_1, π_2, π_3) consists of a number of bases with a deformable configuration. We show two random instances for each texton, and each base is symbolically represented by a bar. This work can learn automatically a second level vocabulary $\mathcal{D}_2$, like stars, birds, cheetah blobs, snowflakes, etc, shown in figure 16. It is expected that natural images have levels of vocabularies with sizes $|\mathcal{D}_1| = O(10)$ and $|\mathcal{D}_2| = O(10^3)$, like the number of phonemes and words in language.

8 Causal Markov Models

Now we discuss the third type of models – causal Markov models which are special cases of descriptive models for computational convenience.

Let $s = (s_1, ..., s_n)$ be the representation of a pattern, and $p_{\text{des}}(s; \boldsymbol{\beta})$ its descriptive model. As Figure 2.b illustrates, a causal Markov model imposes a partial order in the vertices and thus factorizes the joint probability into a product of conditional probabilities,

$$p_{\text{cau}}(s; \boldsymbol{\beta}) = \prod_{i=1}^{n} p(s_i \mid \text{parent}(s_i); \beta_i). \tag{28}$$

parent(s_i) is the set of parent vertices which point to s_i. Though the graph is directed in syntax, it is not a generative model because the variables are at the same semantic level. $p_{\text{cau}}(s)$ can be derived from the minimax entropy learning scheme in Section (4.1).

$$p^*_{\text{cau}} = \arg\max - \sum_s p_{\text{cau}}(s) \log p_{\text{cau}}(s).$$

Thus $p_{\text{cau}}(s; \boldsymbol{\beta})$ is a special class of descriptive model, only the features ϕ_k must be between s_i and parent$(s_i), i = 1, 2, ..., n$, and the constraints are put on the conditional probabilities. When the

dimension of $p(s_i \mid \text{parent}(s_i))$ is not high, (e.g. $|\text{parent}(s_i)| + 1 \leq 4$), the conditional probability are often estimated by a non-parametric Parzen window.

There are many causal Markov models for texture in the 1980s and early 1990s (See Popat and Picard, 1994 and references therein). In the following, we review two pieces of interesting work appeared recently.

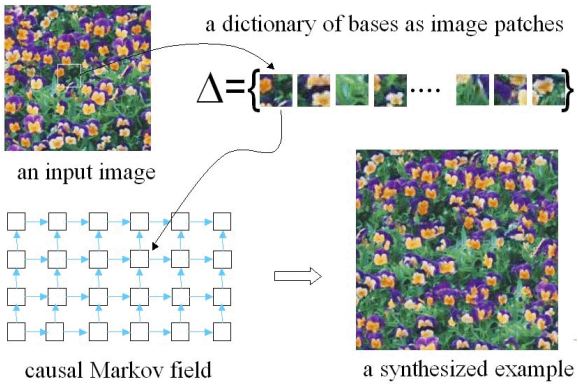

Figure 17: A causal MRF model for example-based texture synthesis.

One is the work on example-based texture synthesis by Efros and Leung (1999), Liang et al. (2001), and Efros and Freeman (2001). Hundred of realistic textures can be synthesized by a patching technique. Figure 17 re-formulates the idea in a causal Markov model. An example texture image is first chopped into a number of image patches of a pre-defined size. These patches form a vocabulary $\mathcal{D}_1 = \Delta$ of image "bases" specific to this texture. Then a causal Markov field is set up with each element being chosen from Δ conditional on two other previous patches (left and below). The patches are pasted one by one in a linear order by sampling from a non-parametric conditional distribution. A synthesized image is shown to the lower-right side. The vocabulary Δ greatly reduces the search space and thus the causal model can be simulated extremely fast (in less then 1 second per image). But the model is biased by the dictionary which is quite large and is not generic model for image analysis.

a). input b). image sketch c). a synthesized sketch.

Figure 18: A causal Markov model for texture sketch. After (Wu et al. 2002).

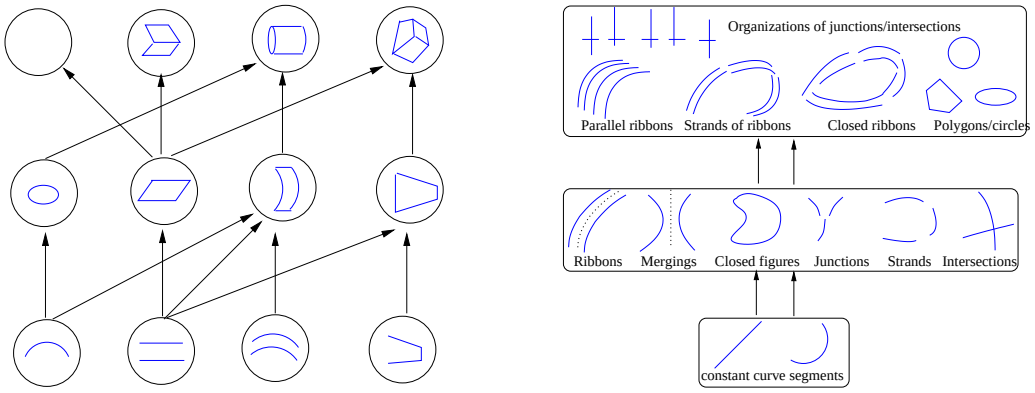

Figure 19: Hierarchic perceptual grouping. a). After (Dickinson et al. 1992) b). After (Sarkar and Boyer, 1994)

A more general causal Markov model was proposed by (Wu et al. ECCV 2002). Wu et.al. represent an image by a number of bases from a generic base dictionary (Log. DoG. DooG) as in sparse coding model. Each base is then symbolically represented by a line segment, as Figures 18.a-b show. This forms a base map similar to the texton (attributed point) pattern in Figure 7. Then a causal model is learned based on Figure 18.b for the base map. The graph structure is more flexible than the grid in Figure 17. A random sample is drawn from the model and shown in Figures 18.c.

When the causal Markov model is integrated with generative models, then the whole graph is still a DAG with random structures, and thus can be compute effectively. Obviously the causal models lose information and can be suboptimal in representation.

9 Discriminative models

Most of the perceptual grouping work (research stream 3) fall in category 4 – discriminative models. (Boyer and Sarkar, 1999) surveyed the literature in perceptual organization comprehensively, so there is no need for an extensive review from us. In this section, we briefly mention some typical work, and then focus on the theoretical connections between discriminative models to the descriptive and generative models.

9.1 Some typical discriminative models

The objective of perceptual grouping is to compose image elements into larger and larger structures in a hierarchy. Figure 19 shows two influential work in the literature. (Dickinson et al, 1992) adopted a hierarchic Bayesian network for grouping short line and curve segments into generic object facets, and the latter are further grouped into 2D views of 3D object parts. (Sarkar and Boyer, 1994) used the Bayesian network for grouping edge elements into hierarchic structures in aerial images. More recent work is (Amir and Lindenbaum, 1999).

If we represent the hierarchic representation by a linear order for ease of discussion, the grouping proceeds from images $\mathbf{I}$ to edge elements W_1, to line and curve segments W_2, to surface and objects, and so on – exactly in the inverse order of the generative model (see equation (19). Figure 2).

$$\mathbf{I} \longrightarrow W_1 \longrightarrow W_2 \longrightarrow \cdots \longrightarrow W_L \tag{29}$$

As the grouping must be done probabilistically, both (Dickinson et al. 1992) and (Sarkar and Boyer, 1994) adopted a list of conditional probabilities in their Bayesian networks. Reformulated in the above notation, they are,

$$q(W_1|\mathbf{I}), \quad q(W_2|W_1), \quad ..., \quad q(W_L|W_{L-1}).$$

Again, we use linear order here for clarity. There may be express-ways for computing objects from edge elements directly, such as generalized Hough transform. In the literature, most of these conditional probabilities are manually estimated or calculated in a similar way to (Lowe, 1987).

9.2 The computational role of discriminative models

The discriminative models for grouping are demonstrated effective and useful in vision. However, there are a number of conceptual problems suggesting that they should perhaps not be considered *representational models*, instead they are *computational models*. In the desk example of Figure 2, (or similarly in the hierarchies shown in figure 19), the presence of a leg may, as a piece of evident, "suggests" the presence of a desk but it does not "cause" a desk. A leg can also suggest chairs and a dozen other types of furniture which have legs. It is the desk concept that causes 4 legs and a top at various configurations in the generative model.

What is wrong with the inverted arrows in discriminative models? A key point associated with Bayes (causal, belief) networks is the idea of "explaining-away" or "lateral inhibition" in a neuroscience term. If there are multiple competing causes for a symptom, then the recognition of one cause will suppress the other causes. In a generative model, if a leg is recognized as belonging to a desk during computation, then the probability of a chair at the same location is reduced drastically. But in a discriminative model, it appears that the four legs are competing causes for the desk, then one leg should drive away the other three legs in explanation! This is not true. The lack of such an "explaining-away" mechanism creates combinatorial explosions. Because a pixel or an edge can "cause" any objects in the world.

In the Bayesian framework, as well as in EM-learning (see equation (21)), the generative models are a sequence of likelihoods $p(\mathbf{I}|W_1)$, $p(W_1|W_2)$, ..., $p(W_{L-1}|W_L)$. In contrast, the discriminative models are approximations to the posteriors in,

$$q(W_1|\mathbf{I}) \sim p(W_1|\mathbf{I}; \mathcal{D}_1, \boldsymbol{\beta}_0), \quad \cdots, \quad q(W_L|W_{L-1}) \sim p(W_L|W_{L-1}; \mathcal{D}_L, \boldsymbol{\beta}_{L-1}). \tag{30}$$

Like most pattern recognition methods, the approximative posteriors q use only local deterministic features at each level. For example, suppose W_1 is an edge map, then it is usually assumed

that $q(W_1|\mathbf{I}) = q(W_1|\Phi_1(\mathbf{I}))$ with $\Phi_1(\mathbf{I})$ being some local edge measures. For the other levels, $q(W_{I+1}|W_i) = q(W_{i+1}|\Phi_i(W_i))$ with $\Phi_i(W_i)$ being some *compatibility functions and metrics* (Sarkar and Boyer 1994, Bienenstock et al 1997).

For ease of notation, we only consider one level of approximation: $q(W|\mathbf{I}) = q(W|\Phi(\mathbf{I})) \approx p(W|\mathbf{I}; \mathcal{D}, \boldsymbol{\beta})$. By using local and deterministic features, information is lost in each approximation. The amount of information loss is measured by the Kullback-Leibler divergence. Therefore, the best set of features is chosen to minimize the loss.

$$\Phi^* = \arg\min_{\Phi \in \text{Bank}} KL(p \,||\, q) = \arg\min_{\Phi \in \text{Bank}} \sum_{W} p(W|\mathbf{I}; \mathcal{D}, \boldsymbol{\beta}) \log \frac{p(W|\mathbf{I}; Dict, \boldsymbol{\beta})}{q(W|\Phi(\mathbf{I}))}$$

Now we have the following theorem for what are most informative features.[5]

Theorem 5 *For linear features Φ, the divergence $KL(p \,||\, q)$ is equal to the mutual information between variables W and image $\mathbf{I}$ minus the mutual information between W and $\Phi(\mathbf{I})$.*

$$KL(p(W|\mathbf{I}; Dict, \boldsymbol{\beta}) \,||\, q(W|\Phi(\mathbf{I}))) = MI(W, \mathbf{I}) - MI(W, \Phi(\mathbf{I})).$$

$MI(W, \mathbf{I}) = MI(W, \Phi(\mathbf{I}))$ if and only if $\Phi(\mathbf{I})$ is the sufficient statistics for W.

This theorem leads to the *maximum mutual information principle* for feature selection ,

$$\Phi^* = \arg\max_{\Phi \in \text{Bank}} MI(W, \Phi(\mathbf{I})) = \arg\min_{\Phi \in \text{Bank}} KL(p(W|\mathbf{I}; \mathcal{D}, \boldsymbol{\beta}) \,||\, q(W|\Phi(\mathbf{I})))$$

The discriminative models can be used as *importance proposal probabilities* for sampling the hidden variables. This is crucial for both Bayesian inference and for learning generative models (see the E-step in equation (22)). In both tasks, we need to draw samples from the posteriors through Markov chain Monte Carlo (MCMC) techniques. These posteriors are approximated by the discriminative models (see eq.(30)). The convergence of MCMC critically depend on the importance proposal probabilities q. This is stated in the theorem below by (Mengersen and Tweedie, 1994)

Theorem 6 *Sampling a target density $p(x)$ by independence Metropolis-Hastings algorithm with proposal probability $q(x)$. Let $P^n(x_o, y)$ be the probability of a random walk to reach point y at n steps. If there exists $\rho > 0$ such that,*

$$\frac{q(x)}{p(x)} \geq \rho, \quad \forall x.$$

then the convergence measured by a L_1 norm distance

$$||P^n(x_o, \cdot) - p|| \leq (1 - \rho)^n.$$

This theorem, though on a simple case, states the computational role of discriminative model. The idea of using discriminative models, such as edge detection, clustering, Hough transforms, are used in a data-driven Markov chain Monte Carlo (DDMCMC) framework for generic image segmentation, grouping, and recognition (Zhu, Zhang and Tu, CVPR 2000, Tu and Zhu, ICCV 2001, ECCV 2002).

[5] This proof was given in a unpublished report by Wu and Zhu (1999). A similar conclusion was also given by a variational approach by Wolf and George (1999), who sent an unpublished manuscript to Zhu.

10 Discussion

This paper presents an epistemological view of four research streams and four types of vision models. The central theme is to integrate the descriptive models and generative model for modeling and conceptualization of visual patterns. The causal MRF models and discriminative models are effective means for computation. Though the current models are still preliminary, the outline and road map of a unified framework becomes clear. The following are some challenged questions that remains not answered.

1. What is the ultimate goal of learning? Where does it end?

From the perspectives of image coding and learning, the ultimate goal, as stated in Section (3), is to approach the frequency $f(\mathbf{I})$ for the ensemble of natural images. Starting from the raw images, each time when we add a new layer of hidden variables, we make progress in discovering the hidden structures. At the end of this pursuit, suppose we dig out all the hidden variables, then we will have a physically-based model which is the ultimate generative model denoted by p^*_{gen}. This model cannot be further compressed and we reach the Komogorov complexity of the image ensemble.

For example, the chemical diffusion-reaction equations with a few parameters may be the most parsimonious model for rendering some textures. But obviously this is not a model used in human vision. Why didn't human vision pursue such ultimate model? This leads to the second question below.

2. How do you choose a generative model, when there are many possible explanations?

There are two extremes of models. At one extreme, theorem 2 states that the pure descriptive model p^*_{des} on raw pixels, i.e. no hidden variables at all, can approximate the ensemble frequency $f(\mathbf{I})$ as long as we put a huge number of features statistics. At the other extreme end, we have the ultimate generative model p^*_{gen} mentioned above. In graphics, there are also a spectrum of models, ranging from image based rendering to physically-based ray tracing. Certainly our brains choose a model somewhere between p^*_{des} and p^*_{gen}.

We believe that the choice of generative models is decided by two aspects. The first is the purposes of vision for navigation, grasping not just for coding. The second is the computational effectiveness. The former seems hopeless to have a quantitative formulation at present. We only have some understanding on the second issue.

A descriptive model uses features $\Phi()$ which is deterministic and thus easy to compute (filtering) in a bottom-up fashion. But it is very difficult to do synthesis using features. For example, sampling the descriptive model (such as FRAME) is expensive. In contrast, the generative model uses hidden variables W which has to be inferred stochastically and thus expensive to compute (analysis). But it is easier to do top-down synthesis using the hidden variables. For the two extreme models, p^*_{des} is infeasible to sample (synthesis), and p^*_{gen} is infeasible to infer (analysis). For example it is

infeasible to infer parameters of a reaction-diffusion equation from observed texture images. The choice of generative model in the brain should make both analysis and synthesis convenient. Also it is possible that many models have to co-exist due to the diversity of vision tasks.

3. Where do features and hidden variables (i.e. visual vocabulary) come from?

The mathematical principles (minimax entropy or maximum mutual information) can choose "optimal" features and variables from pre-defined sets, but the creation of these candidate sets often come from three sources: 1). observations in human vision, such as psychology and neuroscience, 2). physics models, or 3). artist models. Clearly the three sources have different purposes themselves. Perhaps human vision studies are closer to the truth as human vision systems are general purposed. For example, the Gabor filters, and Gestalt laws are found to be very helpful in visual modeling. At present, the visual vocabulary is still far from being enough.

This may sound ad hoc to someone who likes analytic solutions! Unfortunately, we may never be able to justify such vocabulary mathematically, just as physicists cannot explain why they have to use forces or basic particles and why there are space and time. Any elegant theory starts from assumptions. In this sense, we have to accept that

"The far end of sciences is art".

Acknowledgment

The work is supported by an NSF grant IIS-00-92664 and an ONR grant N-000140-110-535. The author 'd like to thank David Mumford, Yingnian Wu, and Alan Yuille for extensive discussions which lead to the development of this paper, and thank Zhuowen Tu, Cheng-en Guo for their assistance.

References

[1] A. Amir and M. Lindenbaum, "Ground from figure discrimination", *Computer Vision and Image Understanding*, Vol. 76, No.1, pp.7-18, 1999.

[2] J.J. Atick and A.N. Redlich, "What does the retina know about natural scenes?", *Neural Computation*, 4:196-210, 1992.

[3] F. Attneave, "Some informational aspects of visual perception", *Pschological Review*, 61:183-193, 1954.

[4] L. Alvarez, Y. Gousseau, and J-M. Morel, "The size of objects in natural and artificial images", in *Advances in Imaging and Electron Physics*, vol. 111, eds. J-M. Morel, Academic Press, 1999.

[5] H.B. Barlow, "Possible principles underlying the transformation of sensory messages". In *Sensory Communication*, ed. W.A. Rosenblith, pp217-234, MIT Press, Cambridge, MA, 1961.

[6] J. Besag, "Spatial interaction and the statistical analysis of lattice systems (with discussion)." *J. Royal Stat. Soc., B*, **36**, 192-236. 1973.

[7] E. Bienenstock, S. Geman, and D. Potter, "Compositionality, MDL Priors, and Object Recognition", NIPS, 1997.

[8] A. Blake and A. Zisserman. *Visual Reconstruction.* Cambridge, MA. MIT press, 1987.

[9] K.L. Boyer and S. Sarkar, "Perceptual organization in computer vision: status, challenges, and potentials", *Computer Vision and Image Understanding*, Vol. 76, no. 1, pp. 1-5, 1999.

[10] E.J. Candes, Rightlets: Theory and Applications, Ph.D thesis, Stanford University, Statistics, 1998.

[11] C.R. Carlson, "Thresholds for perceived image sharpness", *Photographic Sci. Eng.*, **22**, 69-71, 1978.

[12] D. Chandler, *Introduction to Modern Statistical Mechanics*, Oxford University Press, 1987.

[13] Z.Y. Chi, "Probabilistic models for complex systems", Doctoral dissertation with Stu Geman, Division of Applied Math, Brown University, 1998.

[14] C. Chubb and M.S. Landy, "Othergonal distribution analysis: a new approach to the study of texture perception", in M.S. Landy (eds.) *Comp. Models of visual processing*, Cambridge, MA, MIT Press, 1991.

[15] R.W. Cohen, I. gorog, and C.R. Carlson, "Image descriptors for displays", *Technical Report Cont. No. N00014-74-C-0184*, Office of Navy Research, 1975.

[16] R.R. Coifman and M.V. Wickerhauser, "Entropy based algorithms for best basis selection." *IEEE Trans. on Information Theory.*, Vol.38, pp713-718, 1992.

[17] P. Common, "Independent component analysis — a new concept?", *Signal Processing*, 36, 287-314, 1994.

[18] D. Cooper, "Maximum likelihood estimation of Markov process blob boundaries in noisy images", *IEEE Trans. on PAMI*, vol. 1, pp372-384, 1979.

[19] G. R. Cross and A. K. Jain, "Markov random field texture models", *PAMI*, **5**, 25-39, 1983.

[20] P. Dayan, G. E. Hinton, R. Neal, and R. S. Zemel, "The Helmholtz machine", *Neural Computation*, 7. 1022-1037, 1995.

[21] S. Della Pietra, V. Della Pietra, and J. Lafferty, "Inducing features of random fields", *IEEE Trans. on PAMI*, vol. 19, no.4, April, 1997.

[22] N. G. Deriugin, "The power spectrum and the correlation function of the television signal", *Telecommunications*, **1** (7) 1-12, 1957.

[23] S. J. Dickinson, A. P. Pentland, and A. Rosenfeld, "From volumes to views: an approach to 3D object recognition", *CVGIP: Image Understanding*, Vol.55, No.2, pp. 130-154, March 1992.

[24] D.L. Donoho, M. Vetterli, R.A. DeVore, and I. Daubechie, "Data compression and harmonic analysis", *IEEE Trans. Information Theory.* 6, 2435-2476, 1998.

[25] A. Efros and T. Leung, "Texture synthesis by non-parametric sampling", *Proc. of ICCV*, 1999.

[26] A. Efros and W. T. Freeman, "Image Quilting for Texture Synthesis and Transfer", *SIGGRAPH*, 2001.

[27] D.J. Field, "Relations between the statistics and natural images and the responses properties of cortical cells", *J. Optical Society of America*, A 42379-2394, 1987.

[28] D.J. Field, "What is the goal of sensory coding?", *Neural Computation.* 6, 559-601, 1994.

[29] B. Frey and N. Jojic, "Transformed component analysis: joint estimation of spatial transforms and image components", *Proc. of Int'l Conf on Computer Vision*, Corfu, Greece, 1999.

[30] K.S. Fu, *Syntactic Pattern Recognition*, Prentice-Hall, 1982.

[31] W.S. Geisler, J.S. Perry, B.J. Super, D.P. Gallogly, "Edge co-occurence in natural images predicts contour grouping performance", *Vision Research*, 41, pp711-724, 2001.

[32] S. Geman and D. Geman. "Stochastic relaxation, Gibbs distributions and the Bayesian restoration of images". *IEEE Trans. PAMI* **6**. pp 721-741. 1984.

[33] J. W. Gibbs, *Elementary Principles of Statistical Mechanics*. Yale University Press, 1902.

[34] J.J. Gibson, *The Perception of the visual world*, Houghton Mifflin, Boston, 1966.

[35] U. Grenander, *Lectures in Pattern Theory I, II, and III*, Springer, 1976-1981.

[36] U. Grenander, Y. Chow, and K. M. Keenan, *Hands: A Pattern Theoretical Study of Biological Shapes*, Springer-Verlag, New York, 1991.

[37] U. Grenander and A. Srivastava, "Probability models for clutter in natural images", *IEEE trans. on PAMI*. vol. 23, no.4, 2001.

[38] M. G. Gu and F.H. Kong, "A stochastic approximation algorithm with MCMC method for incomplete data estimation problems", *Proc. of National Academy of Sciences*, USA, **95**, pp 7270-7274, 1998.

[39] C. E. Guo, S. C. Zhu, and Y. N. Wu, "Visual learning by integrating descriptive and generative methods", *ICCV*, 2001.

[40] G. Guy and G. Medioni, "Inferring global perceptual contours from local features", *Int'l J. of Comp. Vis.*, 20, 113-133, 1996.

[41] D.W. Jacobs, "Recognizing 3D objects using 2D images", Doctoral dissertation, MIT AI lab. 1993.

[42] E. T. Jaynes, "Information theory and statistical mechanics", *Physical Review* 106, 620-630, 1957.

[43] B. Julesz, "Textons, the elements of texture perception and their interactions", *Nature*, 290, 91-97, 1981.

[44] M. Kass, A. Witkin, and D. Terzopoulos, "Snakes: active contour models", *Proc. of Int'l Conf. on Computer Vision*, London, 1987.

[45] D. Kersten, "Predictability and redundancy of natural images", *J. Opt. Soc. Am.*, A 4(12):2395-2400, 1987.

[46] K. Koffka, *Principles of Gestalt Psychology*, 1935.

[47] A. Koloydenko, *Modeling natural microimage statistics*, Ph.D. Thesis, Dept. of Math and Stat., UMass, Amherst, 2000.

[48] A.B. Lee, J.G.Huang, and D.B. Mumford, "Random collage model for natural images", *Int'l J. of Computer Vision*, oct. 2000.

[49] L. Liang, Liu, Y. Xu, B.N. Guo, H.Y. Shum, "Real-time texture synthesis by patch-based sampling", MSR-TR-2001-40, March 2001. To appear in *Graphics and Its Applications*.

[50] C. Liu, S. C. Zhu, H. Y. Shum, "Learning inhomogeneous Gibbs model of face by minimax entropy", *ICCV*, 2001.

[51] L. D. Lowe, *Perceptual organization and visual recognition*, Kluwer Academic Publishers, 1985.

[52] S. G. Mallat, "A theory for multiresolution signal decomposition: the wavelet representation", *IEEE Trans. on PAMI*, vol.11, no.7, 674-693, 1989.

[53] K.L. Mengersen and R.L. Tweedie, "Rates of convergence of the Hastings and Metropolis algorithms", *Annals of Statistics*, 24:101-121, 1994.

[54] Y. Meyer, "Principe d'incertitude, bases hilbertiennes et algebres d'operateurs", *Bourbaki Seminar*, no.662, 1985-86.

[55] Y. Meyer, "Ondelettes et Operateurs", Hermann, 1988.

[56] L. Moisan, A. Desolneux and J-M. Morel, "Meaningful Alignments" , *IJCV*, vol. 40:1, 7-23, 2000

[57] D. B. Mumford, "Elastica and Computer Vision", in C.L. Bajaj (ed.) *Algebraic Geometry and Its Applications*, Springer-Verlag, New York, 1994.

[58] D. B. Mumford and J. Shah, "Optimal Approximations of Piecewise Smooth Functions and Associated Variational Problems", *Comm. in Pure and Appl. Math.*, vol.42, 1989.

[59] D. B. Mumford, "Pattern Theory: a Unifying Perspective", *Proc. of 1st European Congress of Mathematics*, Birkhauser-Boston, 1994.

[60] D. B. Mumford, "The statistical decsription of visual signals", In ICIAM 95, edited by K.Kirchgassner, O.Mahrenholtz and R.Mennicken, Akademie Verlag, 1996..

[61] D. B. Mumford and B. Gidas, "Stochastic models for generic images", *Quarterly of Applied Math.*, vol. LIX, no. 1, 85-111, 2001.

[62] B. A. Olshausen and D. J. Field, "Sparse coding with an over-complete basis set: A strategy employed by V1?", *Vision Research*, 37:3311-3325, 1997.

[63] M.B. Priestley, *Spectral Analysis and Time Series*, Academic Press, London, 1981.

[64] T. Poggio, V. Torre and C. Koch, "Computational vision and regularization theory", *Nature*, vol. 317, pp 314-319, 1985.

[65] K. Popat and R. W. Picard, "Novel Cluster-Based Probability Model for Texture Synthesis, Classification, and Compression." *Proc. of SPIE Visual Comm. and Image Proc.*, Boston, MA, pp. 756-768, 1993.

[66] J. Portilla and E. P. Simoncelli, "A parametric texture model based on joint statistics of complex wavelet coefficients", *Int'l Journal of Computer Vision.* 40(1):49-71, 2000.

[67] D.L. Ruderman, "The statistics of natural images", *Network: Computation in Neural Systems*, **5**, 517-548, 1994.

[68] D.L. Ruderman, "Origins of scaling in natural images", *Vision Research*, 37:3385-3398, December, 1997.

[69] S. Sarkar and K. L. Boyer, "Integration, inference, and management of spatial information using Bayesian networks: perceptual organization", *IEEE Trans. on PAMI*, vol. 15, No. 3, 1993.

[70] S. Sarkar and K. L. Boyer, *Computing Perceptual Organization in Computer Vision*, World Scientific Pub. Co. Singapore, 1994.

[71] C. Shannon, "A mathematical theory of communication", *Bell System Tech. Journal*, **27**, 1948.

[72] E.P. Simoncelli, W.T. Freeman, E.H. Adelson, D.J. Heeger, "Shiftable multiscale transforms", *IEEE Trans. on Info. Theory*, 38(2): 587-607, 1992.

[73] E.P. Simoncelli and B. A. Olshausen, "Natural image statistics and neural representation", *Annual Rev. Neurosci.*, 24:1193-1216, 2001.

[74] B.J. Smith, "Perceptual organization in a rnadom stimulus", in *Human and Machine Vision*, Eds. A. Rosenfeld, Academic Press, San Diego, 1986.

[75] D. Stoyan, W. S. Kendall, J. Mecke, *Stochastic Geometry and its Applications*, 1985.

[76] D. Terzopoulos, "Multilevel computational process for visual surface reconstruction", *Computer Vision, Graphics, and Image Processing*, 24, 52-96, 1983.

[77] Z.W. Tu, S.C. Zhu, "Image segmentation by Data Driven Markov chain Monte Carlo", *IEEE Trans. on PAMI* vol 24, no.5, May 2002.

[78] Z.W. Tu and S.C. Zhu, "Parsing images into region and curve processes", *Proc. of ECCV*, Copenhagen, Denmark, 2002.

[79] J.H. Van Hateren and D.L. Ruderman, "Independent component analysis of natural image sequences yields spatiotemproal filters similar to simple cells in primary visual cortex", *Proc. Royal Soc. of London.* 265, 1998.

[80] L. R. Williams and D. W. Jacobs, "Stochastic completion fields: a neural model of illusory contour shape and salience", *Neural Computation*, 9, 837-858, 1997.

[81] D. R. Wolf and E.I. George, "Maximally informative statistics", Unpublished manuscript, 1999.

[82] Y. N. Wu and S. C. Zhu "Equivalence of Julesz and Gibbs Ensembles", *Proc. of ICCV*, Corfu, Greece, 1999.

[83] Y.N. Wu, S.C. Zhu, and C.E. Guo, "Statistical modeling of image sketch", Submitted to ECCV, 2002.

[84] J.S. Yedidia, W.T. Freeman and Y. Weiss, "Generalized belief propagation", TR-2000-26, Mitsubishi Elec. Res. Lab., 2000

[85] A. L. Yuille, "Deformable templates for face recognition", *J. of Cognitive Neuroscience*, vol.3 (1), 1991.

[86] A. L. Yuille, J. M. Coughlan, Y. N. Wu, and S. C. Zhu, "Order Parameter for Detecting Target Curves in Images: How Does High Level Knowledge Helps?", *Int'l Journal of Computer Vision*, vol. 41, No. 1/2, pp.9-33, 2001.

[87] A.L. Yuille, "CCCP Algorithms to Minimize the Bethe and Kikuchi Free Energies: Convergent Alternatives to Belief Propagation". *Neural Computation*, 2001.

[88] S. C. Zhu, Y. N. Wu and D. B. Mumford, "Minimax entropy principle and its application to texture modeling", *Neural Computation* Vol. 9, no 8, Nov. 1997.

[89] S.C. Zhu and D.B. Mumford, "Prior learning and Gibbs reaction-diffusion", *IEEE Trans. PAMI*, vol.19, no.11, Nov. 1997.

[90] S.C. Zhu, Y. N. Wu and D. B. Mumford, "Filters, Random fields, And Maximum Entropy (FRAME): towards a unified theory for texture modeling", *Int'l Journal of Computer Vision*, 27(2) 1-20, 1998. (First appeared in CVPR96).

[91] S. C. Zhu, "Embedding Gestalt laws in Markov random fields", *IEEE Trans. on PAMI.* vol. 21, no.11, 1999.

[92] S.C. Zhu, X.W. Liu, and Y.N. Wu, "Exploring Julesz Texture Ensemble by Effective Markov Chain Monte Carlo", *IEEE Trans. PAMI*, vol. 22, no.6, 2000.

[93] S. C. Zhu, R. Zhang, and Z. W. Tu, "Integrating top-down/bottom-up for object recognition by DDMCMC", *Proc. of CVPR*, Hilton Head, SC, 2000.

[94] S.C. Zhu, C.E. Guo, Y.N. Wu, and Y.Z. Wang, "What are textons", *Proc. of ECCV*, Copenhagen, Denmark, 2002.